Simple modular invariant model for quark, lepton, and flavored QCD axion

Y. H. Ahn[1,*] and Sin Kyu Kang[1,2,†]

[1]*Institute for Convergence Fundamental Study, Seoul National University of Science and Technology, Seoul 139-743, Korea*
[2]*School of Liberal Arts, Seoul National University of Science and Technology, Seoul 139-743, Korea*

We propose a minimal extension of the Standard Model by incorporating sterile neutrinos and a QCD axion to account for the mass and mixing hierarchies of quarks and leptons and to solve the strong CP problem and by introducing $G_{SM} \times \Gamma_N \times U(1)_X$ symmetry. We demonstrate that the Kähler transformation corrects the weight of modular forms in the superpotential and show that the model is consistent with the modular and $U(1)_X$ anomaly-free conditions. This enables a simple construction of a modular-independent superpotential for scalar potential. Using minimal supermultiplets, we demonstrate a level-3 modular form-induced superpotential. Sterile neutrinos explain small active neutrino masses via the seesaw mechanism and provide a well-motivated $U(1)_X$-breaking scale, whereas gauge singlet scalar fields play crucial roles in generating the QCD axion, heavy neutrino mass, and fermion mass hierarchy. The model predicts a range for the $U(1)_X$-breaking scale from 10^{13} to 10^{15} GeV for 1 TeV $< m_{3/2} < 10^6$ TeV. In the supersymmetric limit, all Yukawa coefficients in the superpotential are given by complex numbers with an absolute value of unity, implying a democratic distribution. Performing numerical analysis, we study how model parameters are constrained by current experimental results. In particular, the model predicts that the value of the quark Dirac CP phase falls between 38° to 87°, which is consistent with experimental data, and the favored value of the neutrino Dirac CP phase is around 250°. Furthermore, the model can be tested by ongoing and future experiments on axion searches, neutrino oscillations, and $0\nu\beta\beta$ decay.

I. INTRODUCTION

Despite being theoretically self-consistent and successfully demonstrating experimental results in low-energy experiments so far, the Standard Model (SM) of particle physics leaves unanswered questions in theoretical and cosmological issues and fails to explain some physical phenomena such as neutrino oscillations, muon $g - 2$, etc. Various attempts have been made to extend the SM in order to address these questions and account for experimental results that cannot be explained within the SM. For instance, the canonical seesaw mechanism [1] has been proposed to explain the tiny masses of neutrinos by introducing new heavy neutral fermions alongside the SM particles. Additionally, the Peccei-Quinn (PQ) mechanism [2] has been suggested to solve the strong CP

problem in QCD by extending the SM to include an anomalous $U(1)_X$ symmetry.

Recently, Feruglio [3] proposed a new idea regarding the origin of the structure of lepton mixing. He applied modular invariance[1] under the modular group to determine the flavor structure of leptons without introducing a number of scalar fields. This approach requires the Yukawa couplings among twisted states to be modular forms. It is a string-derived mechanism that naturally restricts the possible variations in the flavor structure of quarks and leptons, which are unconstrained by the SM gauge invariance. However, explaining the hierarchies of the masses and mixing in the quark and lepton sectors remains a challenge. As studied in most references [5], the Yukawa coefficients are assumed to be free parameters[2] which can be determined by matching them with experimental data on fermion mass and mixing hierarchies. This approach is not significantly different from that in the SM, except for the introduction of modular forms. Alternatively, it is also possible to take the Yukawa coefficient to be of order unity, accommodating the hierarchies of

*[*]axionahn@naver.com
[†]skkang@seoultech.ac.kr

---

[1]Modular invariance was analyzed for supersymmetric field theories in Ref. [4].

[2]In Ref. [6], the Yukawa coefficients are assumed to be of order unity.

the fermion masses and mixing. Recently, Ref. [7] has demonstrated that the vanishing QCD angle, a large Cabibbo-Kobayashi-Maskawa (CKM) phase, and the reproduction of quark and lepton masses and mixings can be achieved by using coefficients up to order 1; see also Ref. [8].

To incorporate sterile neutrinos and a QCD axion into the SM and provide a natural explanation for the mass and mixing hierarchies of quarks and leptons, we propose an extension of a modular invariant model based on the four-dimensional (4D) effective action derived from superstring theory with $G_{\rm SM} \times \Gamma_N \times U(1)_X$ symmetry. The non-Abelian discrete symmetry Γ_N with $N = 2, 3, 4, 5$ plays a role of modular invariance and may originate from superstring theory in compactified extra dimensions, where it acts as a finite subgroup of the modular group [9]. To ensure the validity of a modular invariant model with $G_{\rm SM} \times \Gamma_N \times U(1)_X$, we take the followings into account:

(i) T-duality relates one type of superstring theory to another, and it also appears in the 4D low-energy effective field theory derived from superstring theory (for a review, see Ref. [10]). In particular, 4D low-energy effective field theory of type-IIA string theory with a certain compactification is invariant under the modular transformation of the modulus τ,

$$\tau \to \gamma\tau = \frac{a\tau + b}{c\tau + d}, \quad (a, b, c, d \in Z, ad - bc = 1). \quad (1)$$

So, the 4D action we consider is required to be invariant under the modular transformation and gauged $U(1)_X$ symmetry as well as the Kähler transformation [refer to Eq. (9)]. This is necessary to cancel out the modular anomaly (see Ref. [11]) associated with the modular transformation (1) under the nonlocal modular group Γ_N and the gauged $U(1)_X$ anomaly, at the quantum level.

(ii) While type-II string theory allows for low axion decay constant models via D-branes, leading to the gauged $U(1)_X$ that becomes a global PQ symmetry when the $U(1)_X$ gauge boson is decoupled [12], heterotic string theory typically has a $U(1)_X$-breaking scale with a decay constant close to the string scale. The broken $U(1)_X$ gauge symmetry leaves behind a protected global $U(1)_X$ that is immune to quantum-gravitational effects, achieved via the Green-Schwarz (GS) mechanism [13]. The PQ-breaking scale, or the low axion decay constant, can be determined by taking into account both supersymmetry (SUSY)-breaking effects [14] and supersymmetric next-leading-order Planck-suppressed terms [15–17].

The model features a minimal set of fields that transform based on representations of $G_{\rm SM} \times \Gamma_N \times U(1)_X$ and includes modular forms of level N. These modular forms act as Yukawa couplings and transform under the modular group Γ_N. It should be noted that the Kähler transformation [refer to Eq. (9)] corrects the weight of modular forms in the superpotential due to the modular invariance of both the superpotential and Kähler potential; see Eq. (20). This enables a simple construction of a τ-independent super-potential for scalar potential. The so-called flavored-PQ symmetry $U(1)_X$ guarantees the absence of bare mass terms [18]. We minimally extend the model by incorporating three right-handed neutrinos N^c and SM gauge singlet scalar fields $\chi(\tilde{\chi})$. The scalar fields with a modular weight of zero and charged by $+(-)$ under $U(1)_X$ play a crucial role in generating the QCD axion, heavy neutrino mass, and fermion mass hierarchy. Then, the complex scalar field $\mathcal{F} = \chi(\tilde{\chi})$ with modular weight zero acts on dimension-4 (dimension-3) operators well sewn by $G_{\rm SM} \times \Gamma_N \times U(1)_X$ and modular invariance with different orders, which generate the effective interactions for the SM and the right-handed neutrinos as follows:

$$\tilde{c}_1 \mathcal{O}_3(\mathcal{F})^1 + \mathcal{O}_4 \sum_{n=0}^{\rm finite} c_n \left(\frac{\mathcal{F}}{\Lambda}\right)^n + \cdots \quad (2)$$

Here, Λ is the scale of flavor dynamics above which unknown physics exists as a UV cutoff, and Yukawa coefficients $c_n(\tilde{c}_1)$ are all complex numbers assumed to have a unit absolute value ($|\tilde{c}_1|, |c_n| = 1$). The dimension-4 (dimension-3) operators $\mathcal{O}_{4(3)}$ are determined by $G_{\rm SM} \times \Gamma_N \times U(1)_X$ and modular invariance in the supersymmetric limit. These operators include modular forms of level N, which transform according to the representation of Γ_N [3]. We will demonstrate that any additive finite correction terms, which could potentially be generated by higher weight modular forms, are prohibited due to the modular weight of the $\chi(\tilde{\chi})$ fields being zero. Note that there exist the infinite series of higher-dimensional operators induced solely by the combination of $\chi\tilde{\chi}$ in the supersymmetric limit. These operators, represented by dots in Eq. (2), can be absorbed into the finite leading-order terms and effectively modify the coefficients $\tilde{c}_1$ and c_n at the leading order. Furthermore, to avoid the breaking effects of the axionic shift symmetry caused by gravity that spoil the axion solution to the strong CP problem [19], we imposed a $U(1)_X$-mixed gravitational anomaly-free condition [17,20,21].

The rest of this paper is organized as follows. The next section discusses modular and $U(1)_X$ anomaly-free conditions under $G_{\rm SM} \times \Gamma_N \times U(1)_X$ symmetry, along with the modular forms of superpotential corrected by Kähler transformation. Section III presents an example of a superpotential induced by level-3 modular forms. We introduce minimal supermultiplets to address the challenges of tiny neutrino masses, the strong CP problem and the hierarchies of SM fermion mass and mixing. For our purpose, we show how to derive Yukawa

superpotentials and a modular-independent superpotential for the scalar potential and determining the relevant $U(1)_X$ PQ symmetry-breaking scale (or seesaw scale). Additionally, we provide comments on the modular invariant model. In Sec. IV, we visually demonstrate the interconnections between quarks, leptons, and a flavored-QCD axion. In Sec. V, we present numerical values of physical parameters that satisfy the current experimental data on flavor mixing and mass for quarks and leptons while also favoring the assumption in Eq. (2). The study predicts the Dirac CP phases of quarks and leptons as well as the mass of the flavored-QCD axion and its coupling to photons and electrons. The final section provides a summary of our work.

II. MODULAR AND U(1) ANOMALY FREE

T-duality relates different types of superstring theory and is also present in the 4D low-energy effective field theory derived from superstring theory (see Ref. [10] for a review). In particular, type-IIA intersecting D-brane models are related to magnetized D-brane models through T-duality [10]. The group $\Gamma(N)$ acts on the complex variable τ, varying in the upper-half complex plane $\mathrm{Im}(\tau) > 0$, as the modular transformation Eq. (1). Then, the low-energy effective field theory of type-IIA intersecting D-brane models must have the symmetry under the modular transformation (1). First, we shortly review the modular symmetry. The infinite groups $\Gamma(N)$, called principal congruence subgroups of level $N = 1, 2, 3, …$, are defined by

$$\Gamma(N) = \left\{ \begin{pmatrix} a & b \\ c & d \end{pmatrix} \in SL(2, Z), \begin{pmatrix} a & b \\ c & d \end{pmatrix} \right.$$
$$\left. = \begin{pmatrix} 1 & 0 \\ 0 & 1 \end{pmatrix} \pmod{N} \right\}, \tag{3}$$

which are normal subgroups of homogeneous modular group $\Gamma \equiv \Gamma(1) \simeq SL(2, Z)$, where $SL(2, Z)$ is the group of 2×2 matrices with integer entries and determinant equal to 1. The projective principal congruence subgroups are defined as $\bar{\Gamma}(N) = \Gamma(N)/\{\pm I\}$ for $N = 1, 2$. For $N \geq 3$, we have $\bar{\Gamma}(N) = \Gamma(N)$ because the elements $-I$ do not belong to $\Gamma(N)$. The modular group $\bar{\Gamma} \equiv \Gamma/\{\pm I\}$ is generated by two elements S and T,

$$S: \tau \to -\frac{1}{\tau}, \quad T: \tau \to \tau + 1, \tag{4}$$

satisfying

$$S^2 = (ST)^3 = (TS)^3 = \mathbf{1}. \tag{5}$$

They can be represented by the $PSL(2, Z)$ matrices

$$S = \begin{pmatrix} 0 & 1 \\ -1 & 0 \end{pmatrix}, \quad T = \begin{pmatrix} 1 & 1 \\ 0 & 1 \end{pmatrix}. \tag{6}$$

The groups Γ_N are finite modular groups obtained by imposing the condition $T^N = \mathbf{1}$ in addition to Eq. (5), where $\Gamma_N \equiv \bar{\Gamma}/\bar{\Gamma}(N)$. The groups Γ_N are isomorphic to the permutation groups S_3, A_4, S_4, and A_5 for $N = 2, 3, 4, 5$, respectively [9].

We work in the 4D $\mathcal{N} = 1$ string-derived supergravity framework defined by a general Kähler potential $G(\Phi, \bar{\Phi})$ of the chiral superfields Φ and their conjugates,

$$G(\Phi, \bar{\Phi}) = \frac{K(\Phi, \bar{\Phi})}{M_P^2} + \ln \frac{|W(\Phi)|^2}{M_P^6}, \tag{7}$$

and by an analytic gauge kinetic function $f(\Phi)$ of the chiral superfields Φ, where $M_P = (8\pi G_N)^{-1/2} = 2.436 \times 10^{18}$ GeV is the reduced Planck mass with Newton's gravitational constant G_N, $K(\Phi, \bar{\Phi})$ is a real gauge-invariant function of Φ and $\bar{\Phi}$, and $W(\Phi)$ is a holomorphic gauge-invariant function of Φ. Based on the 4D effective field theory derived from type-IIA intersecting D-brane models, we build a modular-invariant model with minimal chiral superfields transforming according to representations of $G_{\mathrm{SM}} \times \Gamma_N \times U(1)_X$. Here, we assume that the non-Abelian discrete symmetry Γ_N as a finite subgroup of the modular group [3] and the anomalous gauged $U(1)_X$ including the SM gauge symmetry G_{SM} may arise from several stacks on D-brane models [10]. In the 4D global supersymmetry, the most general form of the action can be written as

$$\mathcal{S} = \int d^4x d^2\theta d^2\bar{\theta} K(\Phi, \bar{\Phi}e^{2A}) + \left\{ \int d^4x d^2\theta \left(W(\Phi) + \frac{f_{ab}(\Phi)}{4} \mathcal{W}^{\alpha a} \mathcal{W}_\alpha^b \right) + \mathrm{H.c.} \right\}, \tag{8}$$

where $A \equiv A^a T^a$ is the gauge multiplet containing Yang-Mills multiplet, T^a are the gauge group generators, and $\mathcal{W}_\alpha$ is a gauge-invariant chiral spinor superfield containing the Yang-Mills field strength. The chiral superfields Φ denote all chiral supermultiplets with Kähler moduli, complex structure moduli, axiodilaton, and matter superfields, transforming under $G_{\mathrm{SM}} \times \Gamma_N \times U(1)_X$. We assume that the low-energy Kähler potential K, superpotential W, and gauge kinetic function f for moduli and matter superfields are given at a scale where Kähler moduli and complex structure moduli are stabilized through fluxes (see Refs. [22–24]), leading to a consistent low-energy SM gauge theory.

Under the modular transformation Eq. (1) and the gauged $U(1)_X$ symmetry, the action (8) should be invariant with the transformations[3]

$$K(\Phi, \bar{\Phi}e^{2A}) \to K(\Phi, \bar{\Phi}e^{2A}) + (g(\Phi) + g(\bar{\Phi}))M_P^2,$$
$$W(\Phi) \to W(\Phi)e^{-g(\Phi)},$$
$$f(\Phi)\mathcal{W}^\alpha \mathcal{W}_\alpha \to f(\Phi)\mathcal{W}^\alpha \mathcal{W}_\alpha, \qquad (9)$$

where $g(\Phi) \equiv g(\tau)$ is a function of modulus τ. Then, the given symmetry $G_{SM} \times \Gamma_N \times U(1)_X$ can be violated at the quantum level by (i) an anomalous triangle graph associated with modular transformation Eq. (1) under the nonlocal modular group Γ_N and (ii) anomalous triangle graphs with external states $A_\nu^a A_\rho^b V_{X\mu}$, where A_ν^a and A_ρ^b are gauge bosons of the SM gauge group G_{SM} and V_X^μ is the connection associated with the gauged $U(1)_X$. These anomalies can be canceled by the GS mechanism [13].

A. Modular anomaly-free and modular forms of level N

To demonstrate the invariance of $K(\Phi, \bar{\Phi}e^{2A})$ and $f(\Phi)\mathcal{W}^\alpha \mathcal{W}_\alpha$ of Eq. (8) under the finite modular group Γ_N and the gauged $U(1)_X$, we consider a low-energy Kähler potential[4]:

$$
\begin{aligned}
K = -M_P^2 \ln\bigg\{ &(S + \bar{S} - 3\tilde{c}\ln(-i\tau + i\bar{\tau})) \\
&\times \left(U_X + \bar{U}_X - \frac{\delta_X^{GS}}{16\pi^2} V_X \right) \prod_{i=1}^2 (\mathcal{U}_i + \bar{\mathcal{U}}_i) \bigg\} \\
&- M_P^2 \ln(-i\tau + i\bar{\tau})^3 + (-i\tau + i\bar{\tau})^{-k}|\varphi|^2 \\
&+ Z_X \varphi_X^\dagger e^{-XV_X} \varphi_X + \cdots, \qquad (10)
\end{aligned}
$$

where $-k$ is the modular weight, Z_X is the normalization factor, S denotes the axiodilaton field, τ represents the overall Kähler modulus, and U_X and $\mathcal{U}_i$ correspond to the complex structure moduli. The dots in Eq. (10) denote the contributions of nonrenormalizable terms scaled by an UV cutoff M_P invariant under $G_{SM} \times \Gamma_N \times U(1)_X$. We note that the matter fields φ_X with $U(1)_X$ charge, complex structure modulus U_X, and the vector superfield V_X of the gauged $U(1)_X$ including the gauge field A_X^μ participate in the 4D GS mechanism. We take the holomorphic gauge kinetic function to be linear in the complex structure moduli U_X and $\mathcal{U}_i$, $f_{ab}(\Phi) \supset \delta_{ab}(S + U_X + \mathcal{U}_i)$. These moduli are associated with the SM gauge theory, which we will not be focusing on. The GS parameter δ_X^{GS} characterizes the coupling of the anomalous gauge boson

---

[3]The upper two shifts in Eq. (9) of the Kähler potential and superpotential are known as the "Kähler transformation" with reference to Eq. (7).

[4]It is similar to the one-loop Kähler potential presented in Ref. [11].

---

to the axion θ_X. The matter superfields in K consist of all scalar fields that are not moduli and do not have Planck-sized vacuum expectation values (VEVs). The scalar components of φ and φ_X are neutral under the $U(1)_X$ symmetry and the modular group Γ_N, respectively.

Calculating $K_{IJ} = \partial_I \partial_J$ from the Kähler potential (10), we obtain the kinetic terms for the scalar components of the supermultiplets which are approximated well for $M_P \gg \langle \varphi \rangle, \langle \varphi_X \rangle$ and $V_X = 0$ as

$$
\begin{aligned}
\mathcal{L}_{kinetic} \simeq &\frac{3M_P^2}{\langle -i\tau + i\bar{\tau} \rangle^2} \partial_\mu \bar{\tau} \partial^\mu \tau + \frac{M_P^2}{\langle U_X + \bar{U}_X \rangle^2} \partial_\mu \bar{U}_X \partial^\mu U_X \\
&+ \frac{M_P^2}{\langle S + \bar{S} - 3\tilde{c}\ln(-i\tau + i\bar{\tau}) \rangle^2} \partial_\mu \bar{S} \partial^\mu S \\
&+ K_{\varphi\bar{\varphi}} \partial_\mu \bar{\varphi} \partial^\mu \varphi + K_{\varphi_X \bar{\varphi}_X} \partial_\mu \bar{\varphi}_X \partial^\mu \varphi_X, \qquad (11)
\end{aligned}
$$

where $K_{\varphi\bar{\varphi}} = K_{\varphi_X \bar{\varphi}_X} = 1$ for canonically normalized scalar fields achieved by rescaling the fields φ and φ_X for given values of the VEVs of τ and U_X. The $U(1)_X$ charged modulus U_X and scalar field φ_X can be decomposed as

$$U_X = \frac{\rho_X}{2} + i\theta_X, \quad \varphi_X|_{\theta=\bar{\theta}=0} = \frac{1}{\sqrt{2}} e^{i\frac{A_X}{v_X}}(v_X + h_X), \qquad (12)$$

where $\rho_X/2 = 1/g_X^2$ with g_X being 4D $U(1)_X$ gauge coupling and A_X, v_X, and h_X are the axion, VEV, and Higgs boson of scalar components, respectively. Because of the axionic shift symmetry, the kinetic terms of Eq. (11) for the axionic and size part of U_X do not mix in perturbation theory, where any nonperturbative violations are small enough to be irrelevant, and the same goes for the axion and Higgs boson of the scalar components of φ_X for $v_X \to \infty$.

Since the matter superfields φ and axiodilaton S transform as

$$\varphi \to (c\tau + d)^{-k} \rho(\gamma)\varphi, \qquad S \to S - 3\tilde{c}\ln(c\tau + d), \qquad (13)$$

where $\rho(\gamma)$ is the unitary representation of the modular group Γ_N and $\tilde{c}$ is a constant, the transformation of the Kähler potential K given in Eq. (9) leads us to

$$g(\tau) = \ln(c\tau + d)^3. \qquad (14)$$

Generically, the transformation of K in Eq. (9) incorporating Eq. (14) gives rise to a modular anomaly arising from $\delta S = -\tilde{c}\frac{1}{4}\int d^4x d^2\theta \mathcal{W}^\alpha \mathcal{W}_\alpha g(\tau) + \text{H.c.}$ [11],

$$-\frac{1}{8}\tilde{c}\{(g(\tau) + g(\bar{\tau}))Q^{\mu\nu}Q_{\mu\nu} + i(g(\tau) - g(\bar{\tau}))Q^{\mu\nu}\tilde{Q}_{\mu\nu}\}, \qquad (15)$$

where $\tilde{Q}_{\mu\nu} = \frac{1}{2}\varepsilon_{\mu\nu\rho\sigma}Q^{\rho\sigma}$ with associated gauge field strengths Q and the first term in the brackets represents the kinetic term for gauge bosons and the second term is the

CP-odd term. After receiving a correction due to the modular transformation of S in Eq. (13), The gauge kinetic function f_{ab} is given at leading order by

$$f^{1-\text{loop}}(\Phi) = \delta_{ab}(S + U_X) - \tilde{c}\ln(c\tau + d)^3, \quad (16)$$

where the second term in the right-hand side is the correction. It is worthwhile to notice that this correction cancels the modular anomaly (15) generated by $g(\tau), g(\bar{\tau})$.

The modular invariance $W(\Phi)$ under the modular group Γ_N ($N \geq 2$) provides a strong restriction on the flavor structure [3]. The superpotential $W(\Phi)$ can be expanded in power series of the multiplets φ which are separated into brane sectors $\varphi_{(I)}$,

$$W(\Phi) = \sum_n Y_{I_1...I_n}(\tau)\varphi_{(I_1)} \cdots \varphi_{(I_n)}, \quad (17)$$

where the functions $Y_{I_1...I_n}(\tau)$ are generically[5] τ-dependent in type-IIA intersecting D-brane models [10,26]. The superpotential $W(\Phi)$ must have modular invariance under the transformation $W(\Phi) \to W(\Phi)e^{-g(\tau)}$, where $g(\tau)$ is given by Eq. (14). To ensure this, we need to satisfy two conditions: (i) the matter superfields φ_{I_i} of the brane sector I_i should transform

$$\varphi_{(I_i)} \to (c\tau + d)^{-k_{I_i}}\rho_{(I_i)}(\gamma)\varphi_{(I_i)} \quad (18)$$

in a representation $\rho_{(I_i)}(\gamma)$ of the modular group Γ_N, where $-k_{I_i}$ is the modular weight of sector I_i, and (ii) the functions $Y_{I_1...I_n}(\tau)$ should be modular forms of weight $k_Y(n)$ transforming in the representation $\rho(\gamma)$ of Γ_N,

$$Y_{I_1...I_n}(\gamma\tau) = (c\tau + d)^{k_Y(n)}\rho(\gamma)Y_{I_1...I_n}(\tau), \quad (19)$$

with the requirements

$$k_Y(n) - 3 = k_{I_1} + \cdots + k_{I_n},$$
$$\rho(\gamma) \otimes \rho_{(I_1)} \otimes \cdots \otimes \rho_{(I_n)} \ni \mathbf{1}. \quad (20)$$

The weight of modular forms in the superpotential is corrected by the Kähler transformation in Eq. (9) due to the modular invariance of both the superpotential and Kähler potential. For example, a τ-independent superpotential for scalar potential can be simply constructed by the matter supermultiplets that belong to the untwisted sector in the orbifold compactification of type-II string theory [see Eq. (37)]. We will show an explicit example of the superpotential induced by the modular forms of level 3 in the Sec. III.

---

[5]In type-II string orientifold compactifications, the Yukawa couplings have modular properties [25].

B. Gauged U(1) anomaly free

The 4D action given by Eq. (8) should also be $U(1)_X$ gauge invariant. Under the $U(1)_X$ gauge transformation $V_X \to V_X + i(\Lambda_X - \bar{\Lambda}_X)$, the matter superfields Φ_X and complex structure modulus U_X transform as

$$\Phi_X \to e^{iX\Lambda_X}\Phi_X, \qquad U_X \to U_X + i\frac{\delta_X^{\text{GS}}}{16\pi^2}\Lambda_X, \quad (21)$$

where $\Lambda_X(\bar{\Lambda}_X)$ are (anti)chiral superfields parametrizing $U(1)_X$ transformation on the superspace. So, the axionic modulus θ_X and axion a_X have shift symmetries

$$\theta_X \to \theta_X - \frac{\delta_X^{\text{GS}}}{16\pi^2}\xi_X, \qquad a_X \to a_X + \frac{\delta_X^{\text{GS}}}{\delta_X^Q}f_X\xi_X, \quad (22)$$

where $\xi_X = -\text{Re}\Lambda_X|_{\theta=\bar{\theta}=0}$, $f_X = Xv_X$ is the axion decay constant and δ_X^Q are anomaly coefficients defined in Eq. (25). Then, the $U(1)_X$ gauge field A_X^μ transforms as

$$A_X^\mu \to A_X^\mu - \partial^\mu\xi_X. \quad (23)$$

Since the gauged $U(1)_X$ is anomalous, the axion a_X and axionic modulus θ_X couple to the (non-)Abelian Chern-Pontryagin densities for the SM gauge group in the compactification. In type-II string vacuum, the $U(1)_X$ anomalies should be canceled by appropriate shifts of Ramond-Ramond axions in the bulk [27–30]. The 4D effective action of the axions, θ_X and a_X, and its corresponding gauge field A_X^μ contains [16,31]

$$K_{U_X\bar{U}_X}\left(\partial^\mu\theta_X - \frac{\delta_X^{\text{GS}}}{16\pi^2}A_X^\mu\right)^2 - \frac{1}{4g_X^2}F_X^{\mu\nu}F_{X\mu\nu}$$
$$- g_X\xi_X^{\text{FI}}D_X + D_Xg_XX|\varphi_X|^2 + |D_\mu\varphi_X|^2 + \theta_X\text{Tr}(Q^{\mu\nu}\tilde{Q}_{\mu\nu})$$
$$+ \frac{a_X}{f_X}\frac{\delta_X^Q}{16\pi^2}\text{Tr}(Q^{\mu\nu}\tilde{Q}_{\mu\nu}), \quad (24)$$

where the gauge field strengths $Q = G, W, Y$ for $SU(3)_C$, $SU(2)_L$, and $U(1)_Y$, respectively, and their gauge couplings are absorbed into their corresponding gauge field strengths. $F_X^{\mu\nu}$ is the $U(1)_X$ gauge field strength defined by $F_X^{\mu\nu} = \partial^\mu A_X^\nu - \partial^\nu A_X^\mu$. In $|D_\mu\varphi_X|^2$, the scalar components of φ_X couple to the $U(1)_X$ gauge boson, where the gauge coupling g_X is absorbed into the gauge boson A_X^μ in the $U(1)_X$ gauge covariant derivative $D^\mu = \partial^\mu - iXA_X^\mu$. The coefficients of the mixed $U(1)_X \times [SU(3)_C]^2$, $U(1)_X \times [SU(2)_L]^2$, and $U(1)_X \times [U(1)_Y]^2$ anomalies are given, respectively, by

$$\delta_X^G = 2\text{Tr}[XT_{SU(3)}^2], \quad \delta_X^W = 2\text{Tr}[XT_{SU(2)}^2], \quad \delta_X^Y = 2\text{Tr}[XY^2].$$
$$(25)$$

Here, $U(n)$ generators ($n \geq 2$) are normalized according to $\text{Tr}[T^a T^b] = \delta_{ab}/2$, and for convenience, $\delta_X^Y = 2\text{Tr}[XY^2]$ is defined for hypercharge. The Fayet-Iliopoulos (FI) term $\mathcal{L}_X^{\text{FI}} = -\xi_X^{\text{FI}} \int d^2\theta V_X = -\xi_X^{\text{FI}} g_X D_X$ with $D_X = g_X(\xi_X^{\text{FI}} - X|\varphi_X|^2)$ leads to D-term potential for the anomalous $U(1)_X$,

$$V_D = \frac{1}{U_X + \bar{U}_X}(-\xi_X^{\text{FI}} + X|\varphi_X|^2)^2, \qquad (26)$$

where ξ_X^{FI} is the FI factor produced by expanding the Kähler potential (10) in components linear in V_X and depends on the closed string modulus $\text{Re}[U_X] = \rho_X/2$. Since the FI term is controlled by the string coupling, it cannot be zero. The restabilization of VEVs by φ_X necessarily implies spontaneous breaking of the anomalous $U(1)_X$, which will be shown later.

The first, third, fourth, and fifth terms in Eq. (24) result from expanding the Kähler potential of Eq. (10). The first and sixth terms together, and the fifth and seventh terms in Eq. (24), are gauge invariant under the anomalous $U(1)_X$ gauge transformations of Eqs. (22) and (23). The gauge-invariant interaction Lagrangian is given by

$$\mathcal{L}_{A\theta}^{\text{int}} = -A_X^\mu J_\mu^\theta + \theta_X \text{Tr}(Q^{\mu\nu} \tilde{Q}_{\mu\nu}) - A_X^\mu J_\mu^X$$
$$+ \frac{a_X}{f_X} \frac{\delta_X^Q}{16\pi^2} \text{Tr}(Q^{\mu\nu} \tilde{Q}_{\mu\nu}), \qquad (27)$$

where the anomalous currents J_μ^X and J_μ^θ coupling to the gauge boson A_X^μ [that is, $\partial_\mu J_X^\mu = \frac{\delta_X^{\text{GS}}}{16\pi^2}\text{Tr}(Q^{\mu\nu}\tilde{Q}_{\mu\nu}) = -\partial_\mu J_\theta^\mu$ with $\delta_X^{\text{GS}} = \alpha_X^Q \delta_X^Q$] are represented by $J_\mu^\theta = K_{U_X \bar{U}_X} \frac{\delta_X^{\text{GS}}}{8\pi^2}\partial_\mu\theta_X$ and $J_\mu^X = -iX\varphi_X^\dagger \overset{\leftrightarrow}{\partial}_\mu \varphi_X$.

Expanding Eq. (24) and setting $\theta_X = a_\theta/8\pi^2 f_\theta$ with $f_\theta = \sqrt{\frac{2K_{U_X\bar{U}_X}}{(8\pi^2)^2}}$ to canonically normalize, $\mathcal{L}_{A\theta}^{\text{int}}$ becomes

$$\frac{1}{2}(\partial^\mu a_\theta)^2 + \frac{a_\theta}{8\pi^2 f_\theta}\text{Tr}(Q^{\mu\nu}\tilde{Q}_{\mu\nu}) + \frac{1}{2}(\partial^\mu A_X)^2$$
$$+ \frac{A_X}{f_X}\frac{\delta_X^Q}{16\pi^2}\text{Tr}(Q^{\mu\nu}\tilde{Q}_{\mu\nu}) - A_X^\mu(J_\mu^X + J_\mu^\theta) + \frac{1}{2g_X^2}m_X^2 A_X^\mu A_{X\mu}$$
$$- \frac{1}{4g_X^2}F_X^{\mu\nu}F_{X\mu\nu} - \frac{g_X^2}{2}(\xi_X^{\text{FI}} - X|\varphi_X|^2)^2, \qquad (28)$$

where the gauge boson mass m_X obtained by the super-Higgs mechanism is given by $m_X = \sqrt{2K_{U_X\bar{U}_X}(\delta_X^{\text{GS}}/16\pi^2)^2 + 2f_X^2}$. Then, the open string axion a_X (decay constant f_X) is mixed linearly with the closed string a_θ (decay constant f_θ),

$$\tilde{A} = \frac{a_X\frac{\delta_X^{\text{GS}}}{2}f_\theta - a_\theta f_X}{\sqrt{f_X^2 + (\frac{\delta_X^{\text{GS}}}{2}f_\theta)^2}} \approx a_X, \qquad G = \frac{a_\theta\frac{\delta_X^{\text{GS}}}{2}f_\theta + A_X f_X}{\sqrt{f_X^2 + (\frac{\delta_X^{\text{GS}}}{2}f_\theta)^2}} \approx a_\theta,$$
$$(29)$$

where the approximations are valid under the assumption that f_θ is much larger than f_X. The gauged $U(1)_X$ absorbs one linear combination of a_X and a_θ, denoted G, giving it a string scale mass through the $U(1)_X$ gauge boson, while the other combination, $\tilde{A} \approx a_X$, remains at low energies and contributes to the QCD axion. At energies below the scale m_X, the gauge boson decouples, leaving behind an anomalous global $U(1)_X$ symmetry.

III. MINIMAL MODEL SETUP

For our purpose, we take into account $\Gamma(3)$ modular symmetry, which gives the modular forms of level 3. The group Γ_3 is isomorphic to A_4, which is the symmetry group of the tetrahedron and the finite groups of the even permutation of four objects having four irreducible representations. Its irreducible representations are three singlets $\mathbf{1}, \mathbf{1}'$, and $\mathbf{1}''$ and one triplet $\mathbf{3}$ with the multiplication rules $\mathbf{3} \otimes \mathbf{3} = \mathbf{3}_s \oplus \mathbf{3}_a \oplus \mathbf{1} \oplus \mathbf{1}' \oplus \mathbf{1}''$ and $\mathbf{1}' \oplus \mathbf{1}' = \mathbf{1}''$, where the subscripts s and a denote symmetric and antisymmetric combinations, respectively. Let (a_1, a_2, a_3) and (b_1, b_2, b_3) denote the basis vectors for two $\mathbf{3}$'s. Then, we have

$$(a \otimes b)_{\mathbf{3}_s} = \frac{1}{\sqrt{3}}(2a_1 b_1 - a_2 b_3 - a_3 b_2, 2a_3 b_3 - a_1 b_2 - a_2 b_1, 2a_2 b_2 - a_3 b_1 - a_1 b_3),$$
$$(a \otimes b)_{\mathbf{3}_a} = (a_2 b_3 - a_3 b_2, a_1 b_2 - a_2 b_1, a_3 b_1 - a_1 b_3),$$
$$(a \otimes b)_{\mathbf{1}} = a_1 b_1 + a_2 b_3 + a_3 b_2,$$
$$(a \otimes b)_{\mathbf{1}'} = a_3 b_3 + a_1 b_2 + a_2 b_1,$$
$$(a \otimes b)_{\mathbf{1}''} = a_2 b_2 + a_3 b_1 + a_1 b_3. \qquad (30)$$

The details of the A_4 group are shown in Appendix A. The modular forms $f(\tau)$ of level 3 and weight k, such as Eq. (19), are holomorphic functions of the complex variable τ with well-defined transformation properties

$$f(\gamma\tau) = (c\tau + d)^k f(\tau)\gamma = \begin{pmatrix} a & b \\ c & d \end{pmatrix} \in \Gamma_3 \quad (31)$$

with an integer $k \geq 0$, under the group Γ_3. The three linearly independent weight-2 and level-3 modular forms are given by [3]

$$Y_1(\tau) = \frac{i}{2\pi} \left[\frac{\eta'(\frac{\tau}{3})}{\eta(\frac{\tau}{3})} + \frac{\eta'(\frac{\tau+1}{3})}{\eta(\frac{\tau+1}{3})} + \frac{\eta'(\frac{\tau+2}{3})}{\eta(\frac{\tau+2}{3})} - \frac{27\eta'(3\tau)}{\eta(3\tau)} \right],$$

$$Y_2(\tau) = \frac{-i}{\pi} \left[\frac{\eta'(\frac{\tau}{3})}{\eta(\frac{\tau}{3})} + \omega^2 \frac{\eta'(\frac{\tau+1}{3})}{\eta(\frac{\tau+1}{3})} + \omega \frac{\eta'(\frac{\tau+2}{3})}{\eta(\frac{\tau+2}{3})} \right],$$

$$Y_3(\tau) = \frac{-i}{\pi} \left[\frac{\eta'(\frac{\tau}{3})}{\eta(\frac{\tau}{3})} + \omega \frac{\eta'(\frac{\tau+1}{3})}{\eta(\frac{\tau+1}{3})} + \omega^2 \frac{\eta'(\frac{\tau+2}{3})}{\eta(\frac{\tau+2}{3})} \right], \quad (32)$$

where $\omega = -1/2 + i\sqrt{3}/2$ and $\eta(\tau)$ is the Dedekind eta function defined by

$$\eta(\tau) = q^{1/24} \prod_{n=1}^{\infty} (1 - q^n) \quad \text{with} \quad q \equiv e^{i2\pi\tau} \quad \text{and} \quad \text{Im}(\tau) > 0. \quad (33)$$

The Dedekind eta function satisfies

$$\eta(-1/\tau) = \sqrt{-i\tau}\eta(\tau), \qquad \eta(\tau + 1) = e^{i\pi/12}\eta(\tau). \quad (34)$$

The three linear independent modular functions transform as a triplet of A_4, i.e., $Y_3^{(2)} = (Y_1, Y_2, Y_3)$. The q expansion of $Y_i(\tau)$ reads

$$Y_1(\tau) = 1 + 12q + 36q^2 + 12q^3 + \cdots$$
$$Y_2(\tau) = -6q^{1/3}(17q + 8q^2 + \cdots)$$
$$Y_3(\tau) = -18q^{2/3}(1 + 2q + 5q^2 + \cdots). \quad (35)$$

$Y_3^{(2)}$ is constrained by the relation

$$(Y_3^{(2)}Y_3^{(2)})_{\mathbf{1}''} = Y_2^2 + 2Y_1Y_3 = 0. \quad (36)$$

A. Modular invariant supersymmetric potential and a Nambu-Goldstone mode

Using Eqs. (17)–(20), we construct unique supersymmetric and modular invariant scalar potential by introducing minimal supermultiplets. Those include SM singlet fields χ_0[6] with modular weight 3 and $\chi(\tilde{\chi})$ with modular weight 0. Additionally, we have the usual two Higgs doublets $H_{u,d}$ with modular weight 0, which are responsible for electroweak (EW) symmetry breaking. The fields χ and $\tilde{\chi}$ are charged by $+1$ and -1, respectively, and are

ensured by the extended $U(1)_X$ symmetry due to the holomorphy of the superpotential. (If the seesaw mechanism [1] is implemented, the field χ or $\tilde{\chi}$ may be responsible for the heavy neutrino mass term).

Under $k_I \times A_4 \times U(1)_X$ with the modular weights k_I according to Eq. (20), we assign the two Higgs doublets $H_{u,d}$ to be $(0, \mathbf{1}, 0)$ and three SM gauge singlets $\chi, \tilde{\chi}, \chi_0$ to be $(0, \mathbf{1}, +1)$, $(0, \mathbf{1}, -1)$, $(3, \mathbf{1}, 0)$, respectively.[7] The A_4-singlet χ_0 field with modular weight 3 ensures that the functions $Y_{I_1\ldots I_n}(\tau)$ are independent of τ. The,n the supersymmetric scalar potential invariant under $G_{\text{SM}} \times U(1)_X \times A_4$ is given at leading order by

$$W_v = g_{\chi_0}\chi_0 H_u H_d + \chi_0(g_\chi \chi\tilde{\chi} - \mu_\chi^2), \quad (37)$$

where dimensionless coupling constants g_{χ_0} and g_χ are assumed to be equal to 1 but are modified to Eq. (60) by considering all higher-order terms induced by $\chi\tilde{\chi}$ combinations. Note that the PQ-breaking parameter μ_χ corresponds to the scale of the spontaneous symmetry breaking.

In the global SUSY limit, i.e., $M_P \to \infty$, the scalar potential obtained by the F and D terms of all fields is required to vanish. Then, the relevant F term from Eq. (37) and D term of the scalar potential given by Eq. (26) reads

$$V_F^{\text{global}} = |g_\chi \chi\tilde{\chi} - \mu_\chi^2|^2,$$
$$V_D^{\text{global}} = \frac{|X|^2 g_X^2}{2} \left(-\frac{\xi_X^{\text{FI}}}{|X|} + |\chi|^2 - |\tilde{\chi}|^2 \right)^2. \quad (38)$$

The scalar fields χ and $\tilde{\chi}$ have X charges $+1$ and -1, respectively, i.e.,

$$\chi \to e^{+i\xi}\chi, \qquad \tilde{\chi} \to e^{-i\xi}\tilde{\chi}, \quad (39)$$

with a constant ξ. So, the potential V_{SUSY} has $U(1)_X$ symmetry. Since SUSY is preserved after the spontaneous breaking of $U(1)_X$, the scalar potential in the limit of $M_P \to \infty$ vanishes at its ground states; i.e., $\langle V_F^{\text{global}} \rangle = 0$ as well as $\langle V_D^{\text{global}} \rangle = 0$. From the minimization of the F-term scalar potential, we obtain

$$\langle \chi \rangle = \langle \tilde{\chi} \rangle = \frac{v_\chi}{\sqrt{2}} \quad \text{with} \quad \mu_\chi = v_\chi \sqrt{\frac{g_\chi}{2}}, \quad (40)$$

where we have assumed $\langle \chi \rangle, \langle \tilde{\chi} \rangle \gg \langle H_{u,d} \rangle$. The above supersymmetric solution is taken by the D-flatness condition for [16,17]

---

[6]The field χ_0 can act as an inflaton [16].

[7]As a consequence of $k_I \times A_4 \times U(1)_X$, the other superpotential term $\kappa_\alpha L_\alpha H_u$ and the terms violating the lepton and baryon number symmetries are not allowed. Besides, dimension-6 supersymmetric operators like $Q_i Q_j Q_k L_l$ (where i, j, k must not all be the same) are also not allowed. This restriction is crucial for stabilizing the proton.

$$\xi_X^{\text{FI}} = 0, \qquad \langle \chi \rangle = \langle \tilde{\chi} \rangle. \tag{41}$$

The tension between $\langle \chi \rangle = \langle \tilde{\chi} \rangle$ and $\xi_X^{\text{FI}} \neq 0$ arises because the FI term cannot be canceled, unless the VEV of flux in the FI term is below the string scale [14,32]. The FI term acts as an uplifting potential,

$$\xi_X^{\text{FI}} = M_P^2 \frac{\delta_X^{\text{GS}}}{16\pi^2} \frac{\Delta\rho}{\rho_0}, \tag{42}$$

where $\Delta\rho = \rho_X - \rho_0$, which raises the anti-de Sitter minimum to the de Sitter minimum [14]. To achieve this, the F term must necessarily break SUSY for the D term to act as an uplifting potential. The PQ scale μ_χ can be determined by taking into account both the SUSY-breaking effect, which lifts up the flat direction, and supersymmetric next-leading-order Planck-suppressed terms [15–17]. The supersymmetric next-to-leading-order term invariant under $A_4 \times U(1)_X$ satisfying Eq. (20) is given by

$$\Delta W_v \simeq \frac{\alpha}{M_P^2} \chi_0 (\chi\tilde{\chi})^2, \tag{43}$$

where α is assumed to be a real-valued constant being of unity. Since soft SUSY-breaking terms are already present at the scale relevant to flavor dynamics, the scalar potential for χ, $\tilde{\chi}$ at leading order reads

$$V(\chi, \tilde{\chi}) \simeq -\alpha_1 m_{3/2}^2 |\chi|^2 - \alpha_2 m_{3/2}^2 |\tilde{\chi}|^2 + \alpha^2 \frac{|\chi|^4 |\tilde{\chi}|^4}{M_P^4}, \tag{44}$$

where $m_{3/2}$ represents soft SUSY-breaking mass and α_1 and α_2 are real-valued constants. This leads to the PQ-breaking scale (equivalently, the seesaw scale),

$$\mu_\chi \simeq \left(\frac{g_\chi^6 \alpha_1 \alpha_2}{16\alpha^4} \right)^{\frac{1}{12}} (m_{3/2} M_P^2)^{\frac{1}{3}}, \tag{45}$$

indicating that μ_χ lies within the range of approximately 1.2×10^{13} to 1.7×10^{14} GeV (or 2.6×10^{13} to 1.2×10^{15} GeV) for $m_{3/2}$ values ranging from 1 to 10^3 TeV (or from 10 to 10^6 TeV) for α_1 and α_2 of order unity.

The model includes the SM gauge singlet scalar fields χ and $\tilde{\chi}$ charged under $U(1)_X$, which have interactions invariant under $G_{\text{SM}} \times U(1)_X \times A_4$ with the transformations Eq. (9). These interactions result in a chiral symmetry, which is reflected in the form of the kinetic and Yukawa terms, as well as the scalar potential V_{SUSY} in the SUSY limit,

$$\mathcal{L} \supset \partial_\mu \chi^* \partial^\mu \chi + \partial_\mu \tilde{\chi}^* \partial^\mu \tilde{\chi} + \mathcal{L}_Y - V_{\text{SUSY}} + \mathcal{L}_\vartheta + \bar{\psi} i \partial\!\!\!/ \psi$$
$$+ \frac{1}{2} \bar{N} i \partial\!\!\!/ N + \frac{1}{2} \bar{\nu} i \partial\!\!\!/ \nu, \tag{46}$$

where ψ denotes Dirac fermions and V_{SUSY} is replaced by V_{total} when SUSY-breaking effects are considered. The above kinetic terms for $\chi(\tilde{\chi})$ are canonically normalized from the Kähler potential (10). Here, four component Majorana spinors ($N^c = N$ and $\nu^c = \nu$) are used. The global $U(1)_X$ PQ symmetry guarantees the absence of bare mass term in the Yukawa Lagrangian $\mathcal{L}_Y$ in Eq. (46). The QCD Lagrangian has a CP-violating term

$$\mathcal{L}_\vartheta = \vartheta_{\text{QCD}} \frac{g_s^2}{32\pi^2} G^{a\mu\nu} \tilde{G}_{\mu\nu}^a, \tag{47}$$

where g_s stands for the gauge coupling constant of $SU(3)_C$ and $G^{a\mu\nu}$ is the color field strength tensor and its dual $\tilde{G}_{\mu\nu}^a = \frac{1}{2} \varepsilon_{\mu\nu\rho\sigma} G^{a\mu\nu}$ [here, a is an $SU(3)$-adjoint index], coming from the strong interaction. After obtaining VEV $\langle \chi \rangle \neq 0$, which generates the heavy neutrino masses given by Eq. (53), the PQ $U(1)_X$ symmetry breaks spontaneously at a much higher scale than EW scale. This is manifested through the existence of the Nambu-Goldstone (NG) mode A_X, which interacts with ordinary quarks and leptons via Yukawa interactions; see Eqs. (71), (81), and (92). To extract the associated boson resulting from spontaneous breaking of $U(1)_X$, we set the decomposition of complex scalar fields [17,18,20] as

$$\chi = \frac{v_\chi}{\sqrt{2}} e^{i\frac{A_X}{u_\chi}} \left(1 + \frac{h_\chi}{u_\chi} \right), \qquad \tilde{\chi} = \frac{v_{\tilde{\chi}}}{\sqrt{2}} e^{-i\frac{A_X}{u_\chi}} \left(1 + \frac{h_{\tilde{\chi}}}{u_\chi} \right)$$
$$\text{with} \quad u_\chi = \sqrt{v_\chi^2 + v_{\tilde{\chi}}^2}, \tag{48}$$

in which A_X is the NG mode and we set $v_\chi = v_{\tilde{\chi}}$ and $h_\chi = h_{\tilde{\chi}}$ in the supersymmetric limit. The derivative coupling of NG boson A_X arises from the kinetic term

$$\partial_\mu \chi^* \partial^\mu \chi + \partial_\mu \tilde{\chi}^* \partial^\mu \tilde{\chi} = \frac{1}{2} (\partial_\mu A_X)^2 \left(1 + \frac{h_\chi}{u_\chi} \right)^2 + \frac{1}{2} (\partial_\mu h_\chi)^2. \tag{49}$$

Performing $u_\chi \to \infty$, the NG mode A_X, whose interaction is determined by symmetry, is distinguished from the radial mode h_χ, which is invariant under the symmetry $U(1)_X$.

B. Modular-invariant Yukawa superpotentials and anomaly coefficients

By introducing just two A_4-singlet fields, χ and $\tilde{\chi}$, with modular weight 0 and charged under $U(1)_X$ by $+1$ and -1, respectively, and using economic weight modular forms, we construct Yukawa superpotentials that are invariant under $G_{\text{SM}} \times U(1)_X \times A_4$ satisfying Eq. (20). This approach can explain the observed hierarchy of fermion masses and mixing given by the CKM matrix for quarks as well as by Pontecorvo-Maki-Nakagawa-Sakata (PMNS) matrix for

TABLE I. Representations and quantum numbers of the quark fields under $G_{SM} \times A_4 \times U(1)_X$ and modular weight k_I according to Eq. (20). In $(\mathcal{Q}_1, \mathcal{Q}_2)_Y$ of G_{SM}, $\mathcal{Q}_1$ and $\mathcal{Q}_2$ are the representations under $SU(3)_C$ and $SU(2)_L$ respectively, and the script Y denotes the $U(1)$ hypercharge.

Field	Q_1	Q_2	Q_3	$\mathcal{D}^c$	u^c	c^c	t^c
G_{SM}	$(3,2)_{1/6}$	$(3,2)_{1/6}$	$(3,2)_{1/6}$	$(3,1)_{1/3}$	$(3,1)_{-2/3}$	$(3,1)_{-2/3}$	$(3,1)_{-2/3}$
A_4	$\mathbf{1}$	$\mathbf{1''}$	$\mathbf{1'}$	$\mathbf{3}$	$\mathbf{1}$	$\mathbf{1'}$	$\mathbf{1''}$
k_I	0	0	0	-3	-3	-3	3
$U(1)_X$	$f_b - f_d$	$f_b - f_s$	0	$-f_b$	$f_d - f_b - f_u$	$f_s - f_b - f_c$	0

leptons. Furthermore, the approach provides a solution to the strong CP problem by breaking down the $U(1)_X$ flavor symmetry. Since the modular weights of the fields $\chi(\tilde{\chi})$ are 0, any additive correction terms induced by higher weight modular forms are forbidden in the superpotential [see Eqs. (37), (50), and (53)]. However, higher-order corrections arising from the combination $\chi\tilde{\chi}$ are allowed, but they do not modify the leading-order flavor structure.

Now, let us assign $A_4 \times U(1)_X$ representations and quantum numbers as well as modular weights k_I to the SM quarks and leptons including SM gauge singlet Majorana neutrinos as presented in Table I.[8] Here, three quark $SU(2)_L$ doublets and three up-type quark singlets are denoted as $Q_{i(=1,2,3)}$ and (u^c, c^c, t^c), respectively. $\mathcal{D}^c = \{d^c, s^c, b^c\}$ represents the down-type quark singlets. Then, the quark Yukawa superpotential invariant under $G_{SM} \times A_4 \times U(1)_X$ with modular forms is sewn with $\mathcal{F} = \{\chi \text{ or } \tilde{\chi}\}$ through Eq. (2) as

$$
\begin{aligned}
W_q = {}& \alpha_t^{(0)} t^c Q_3 H_u + \alpha_c^{(0)} \left(\frac{\mathcal{F}}{\Lambda}\right)^{|f_c|} Y_{\mathbf{1}}^{(6)} c^c Q_2 H_u \\
& + \alpha_u^{(0)} \left(\frac{\mathcal{F}}{\Lambda}\right)^{|f_u|} Y_{\mathbf{1}}^{(6)} u^c Q_1 H_u \\
& + \alpha_b^{(0)} \left(\frac{\mathcal{F}}{\Lambda}\right)^{|f_b|} (Y_{\mathbf{3}}^{(6)} \mathcal{D}^c)_{\mathbf{1''}} Q_3 H_d \\
& + \alpha_s^{(0)} \left(\frac{\mathcal{F}}{\Lambda}\right)^{|f_s|} (Y_{\mathbf{3}}^{(6)} \mathcal{D}^c)_{\mathbf{1'}} Q_2 H_d \\
& + \alpha_d^{(0)} \left(\frac{\mathcal{F}}{\Lambda}\right)^{|f_d|} (Y_{\mathbf{3}}^{(6)} \mathcal{D}^c)_{\mathbf{1}} Q_1 H_d + W_q^{(h)},
\end{aligned}
\tag{50}
$$

where $\alpha_i^{(0)}$ denotes coefficient at leading order and $W_q^{(h)}$ stand for higher-order contributions, which are simply constructed by the leading-order operators in Eq. (50) multiplied by $\sum_{n=1}^{\infty} (\frac{\chi\tilde{\chi}}{\Lambda^2})^n$. Note that all Yukawa coefficients in the above superpotential, $\alpha_i^{(0)}$, are assumed to be complex numbers with an absolute value of unity. Since it is hard to reproduce the experimental data of fermion masses and mixing with Yukawa terms constructed with

[8]All fields appearing in Table I are left-handed particles/antiparticles.

modular forms of weight 4 in quark and charged-lepton sectors in this model, we take into account Yukawa terms with modular forms of weight 6 which are decomposed as $\mathbf{1} \oplus \mathbf{3} \oplus \mathbf{3}$ under A_4 given explicitly by [3]

$$
\begin{aligned}
Y_{\mathbf{1}}^{(6)} &= Y_1^3 + Y_2^3 + Y_3^3 - 3Y_1 Y_2 Y_3 \\
Y_{\mathbf{3},1}^{(6)} &= (Y_1^3 + 2Y_1 Y_2 Y_3, \, Y_1^2 Y_2 + 2Y_2^2 Y_3, \, Y_1^2 Y_3 + 2Y_3^2 Y_2) \\
Y_{\mathbf{3},2}^{(6)} &= (Y_3^3 + 2Y_1 Y_2 Y_3, \, Y_3^2 Y_1 + 2Y_1^2 Y_2, \, Y_3^2 Y_2 + 2Y_2^2 Y_1).
\end{aligned}
\tag{51}
$$

In the above superpotential, only the top-quark operator is renormalizable and does not contain a modular form, leading to the top-quark mass as the pole mass, while the other quark operators driven by χ (or $\tilde{\chi}$) are dependent on modular forms. Using modular forms of weight 6, $Y_{\mathbf{1}}^{(6)}$ and $Y_{\mathbf{3}}^{(6)}$, with the quark fields charged under $A_4 \times U(1)_X$, which does not allow mixing among up-type quarks, the off-diagonal entries in the up-type quark mass matrix are forbidden, as indicated in Eq. (65). From the above superpotential, the effective Yukawa couplings of quarks can be visualized as functions of the SM gauge-singlet fields $\chi(\tilde{\chi})$ and modular forms $Y_{\mathbf{1}(\mathbf{3})}^{(6)}$, except for the top Yukawa coupling (see the details given in Sec. IV).

According to the quantum numbers of the quark sectors as in Table I, the color anomaly coefficient of $U(1)_X \times [SU(3)_C]^2$ defined as $N_C \equiv 2\mathrm{Tr}[X_\psi T_{SU(3)_C}^2]$ reads

$$
N_C = -(f_u + f_c + f_d + f_s + f_b).
\tag{52}
$$

Note that $U(n)$ generators ($n \geq 2$) are normalized according to $\mathrm{Tr}[T^a T^b] = \delta^{ab}/2$. The $U(1)_X$ is broken down to its discrete subgroup $Z_{N_{DW}}$ in the backgrounds of the QCD instanton, and the quantity N_C (nonzero integer) is given by the axionic domain-wall number N_{DW}. At the QCD phase transition, each axionic string becomes the edge to N_{DW} domain walls, and the process of axion radiation stops. To avoid the domain-wall problem, one should consider $N_{DW} = 1$ or the PQ phase transition occurred during (or before) inflation for $N_{DW} > 1$.

Next, we turn to the lepton sector, where the fields are charged under $G_{SM} \times A_4 \times U(1)_X$ with modular weight k_I.

TABLE II. Representations and quantum numbers of the lepton fields under $G_{SM} \times A_4 \times U(1)_X$ and modular weight k_I determined according to Eq. (20).

Field	L_e	L_μ	L_τ	e^c	μ^c	τ^c	N^c
G_{SM}	$(1,2)_{-1/2}$	$(1,2)_{-1/2}$	$(1,2)_{-1/2}$	$(1,1)_1$	$(1,1)_1$	$(1,1)_1$	$(1,1)_0$
A_4	$\mathbf{1}$	$\mathbf{1'}$	$\mathbf{1''}$	$\mathbf{1}$	$\mathbf{1''}$	$\mathbf{1'}$	$\mathbf{3}$
k_I	$\frac{5}{2}$	$\frac{5}{2}$	$\frac{5}{2}$	$-\frac{11}{2}$	$-\frac{11}{2}$	$-\frac{11}{2}$	$-\frac{3}{2}$
$U(1)_X$	$\frac{1}{2} - g_e$	$\frac{1}{2} - g_\mu$	$\frac{1}{2} - g_\tau$	$g_e - \frac{1}{2} - f_e$	$g_\mu - \frac{1}{2} - f_\mu$	$g_\tau - \frac{1}{2} - f_\tau$	$-\frac{1}{2}$

Remark that the sterile neutrinos N^c (which interact with gravity) are introduced (i) to solve the anomaly-free condition of $U(1) \times [\text{gravity}]^2$, (ii) to explain the small active neutrino masses via the seesaw mechanism, and (iii) to provide a theoretically well-motivated PQ symmetry-breaking scale. In Table II, the representations and quantum numbers of the lepton fields as well as modular weight k_f determined along with Eq. (20) are presented. Here, L_e, L_μ, and L_τ denote $SU(2)_L$ lepton doublets, and e^c, μ^c, and τ^c are three charged-lepton singlets. The field N^c represents the right-handed $SU(2)_L$ singlet neutrino, which is introduced

to generate active neutrino masses via canonical seesaw mechanism [1].

We note that the mixing between different charged leptons does not occur when the lepton Yukawa superpotential is economically constructed with modular forms of weight 6, resulting in the diagonal form of the charged lepton mass matrix as can be seen in Eq. (78). In contrast, modular forms $Y_{\mathbf{3}}^{(2)}$, $Y_{\mathbf{1}}^{(6)}$, and $Y_{\mathbf{3}}^{(6)}$ are used to construct neutrino mass matrices.[9] Then, the Yukawa superpotential for lepton invariant under $G_{SM} \times A_4 \times U(1)_X$ with economic modular forms are sewn with $\mathcal{F} = \{\chi \text{ or } \tilde{\chi}\}$ through Eq. (2), respectively, as

$$W_{\ell\nu} = \alpha_\tau^{(0)} \left(\frac{\mathcal{F}}{\Lambda}\right)^{|f_\tau|} Y_{\mathbf{1}}^{(6)} \tau^c L_\tau H_d + \alpha_\mu^{(0)} \left(\frac{\mathcal{F}}{\Lambda}\right)^{|f_\mu|} Y_{\mathbf{1}}^{(6)} \mu^c L_\mu H_d + \alpha_e^{(0)} \left(\frac{\mathcal{F}}{\Lambda}\right)^{|f_e|} Y_{\mathbf{1}}^{(6)} e^c L_e H_d + \beta_1^{(0)} \left(\frac{\mathcal{F}}{\Lambda}\right)^{|g_e|} (Y_{\mathbf{3}}^{(2)} N^c)_{\mathbf{1}} L_e H_u$$

$$+ \beta_2^{(0)} \left(\frac{\mathcal{F}}{\Lambda}\right)^{|g_\mu|} (Y_{\mathbf{3}}^{(2)} N^c)_{\mathbf{1''}} L_\mu H_u + \beta_3^{(0)} \left(\frac{\mathcal{F}}{\Lambda}\right)^{|g_\tau|} (Y_{\mathbf{3}}^{(2)} N^c)_{\mathbf{1'}} L_\tau H_u + \gamma_1^{(0)} \frac{1}{2} Y_{\mathbf{1}}^{(6)} (N^c N^c)_{\mathbf{1}} \chi + \gamma_2^{(0)} \frac{1}{2} Y_{\mathbf{3}}^{(6)} (N^c N^c)_{\mathbf{3}} \chi + W_{l\nu}^{(h)},$$

$$(53)$$

where $\alpha_i^{(0)}$, $\beta_i^{(0)}$, and $\gamma_i^{(0)}$ denote coefficients at leading order and $W_{l\nu}^{(h)}$ stands for higher-order contributions triggered by the combination $\chi\tilde{\chi}$. Like in the quark sector, the Yukawa coefficients in the above superpotential, such as $\alpha_i^{(0)}$, $\beta_i^{(0)}$, and $\gamma_i^{(0)}$, are assumed to be complex numbers with an absolute value of unity. In the above superpotential, the charged-lepton and Dirac neutrino parts have three distinct Yukawa terms each, with their common modular forms being $Y_{\mathbf{1}}^{(6)}$ and $Y_{\mathbf{3}}^{(2)}$, respectively. Each term involves $\mathcal{F}/\Lambda$ to the power of an appropriate $U(1)_X$ quantum number. The flavored $U(1)_X$ PQ symmetry allows for two renormalizable terms for the right-handed neutrino N^c, which implement the seesaw mechanism [1] by making the VEV $\langle\chi\rangle$ large. The details on how the active neutrino masses and mixing are predicted will be presented in Sec. IV C.

Nonperturbative quantum gravitational anomaly effects [19] violate the conservation of the corresponding current, $\partial_\mu J_X^\mu \propto R\tilde{R}$, where R is the Riemann tensor and $\tilde{R}$ is its dual, and make the axion solution to the strong CP problem problematic. To consistently couple gravity to

matter charged under $U(1)_X$, the mixed-gravitational anomaly $U(1)_X \times [\text{gravity}]^2$ (related to the color anomaly $U(1)_X \times [SU(3)_C]^2$) must be canceled, as shown in Refs. [17,20,21], which leads to the relation,

$$3N_C = f_e + f_\mu + f_\tau + g_e + g_\mu + g_\tau. \quad (54)$$

Thus, the choice of $U(1)_X$ charge for ordinary quarks and leptons is strictly restricted.

---

[9]By selecting appropriate modular weight of particle contents, lower-weight modular forms can be used, such as $Y_{\mathbf{3}}^{(2)}$ in the Dirac neutrino sector, and $Y_{\mathbf{1}(\mathbf{1'},\mathbf{1''})}^{(4)}$ and $Y_{\mathbf{3}}^{(4)}$ in the Majorana neutrino sector. However, this leads to additional interactions, including $\frac{1}{2} Y_{\mathbf{1}}^{(4)} (N^c N^c)_{\mathbf{1}} \chi$, $\frac{1}{2} Y_{\mathbf{1'}}^{(4)} (N^c N^c)_{\mathbf{1''}} \chi$, $\frac{1}{2} Y_{\mathbf{1''}}^{(4)} (N^c N^c)_{\mathbf{1'}} \chi$, and $\frac{1}{2} Y_{\mathbf{3}}^{(4)} (N^c N^c)_{\mathbf{3}} \chi$. Another option is to use $Y_{\mathbf{3}}^{(2)}$ in the Dirac neutrino sector and no modular form in the Majorana neutrino sector, which results in only $\frac{1}{2} (N^c N^c)_{\mathbf{1}} \chi$ and degenerate heavy Majorana neutrino mass states at the seesaw scale. However, we have found that this approach is difficult to reconcile with experimental neutrino data.
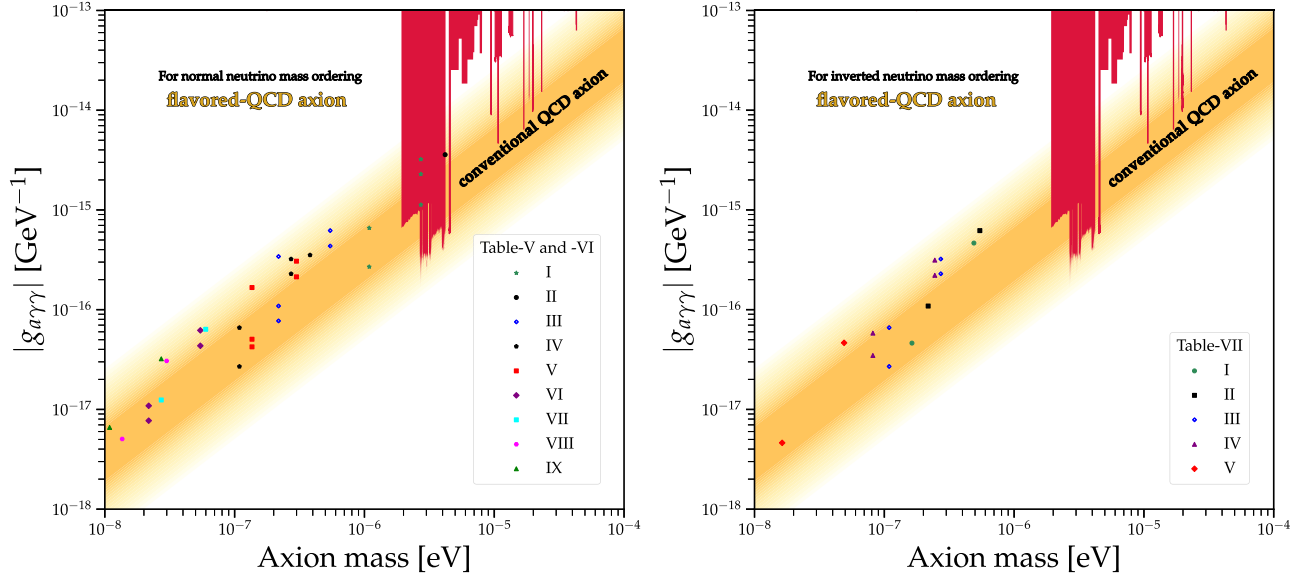
FIG. 1. Plots for axion-photon coupling $|g_{a\gamma\gamma}|$ as a function of the flavored-QCD axion mass m_a for NO and IO. The orange shaded region and vertical red lines indicate the conventional QCD axion predictions and the exclusion region of various axion search experiments, respectively; see Ref. [35].

Below the $U(1)_X$ symmetry-breaking scale (here, equivalent to the seesaw scale), the effective interactions of QCD axion with the weak and hypercharge gauge bosons and with the photon are expressed through the chiral rotation of Eq. (62), respectively, as

$$\mathcal{L}_A^{WY} = \frac{A_X}{f_A} \frac{1}{32\pi^2} \{ g_W^2 N_W W^{\mu\nu} \tilde{W}_{\mu\nu} + g_Y^2 N_Y Y^{\mu\nu} \tilde{Y}_{\mu\nu} \}, \quad (55)$$

$$\mathcal{L}_A^{\gamma} = \frac{A_X}{f_A} \frac{e^2}{32\pi^2} E F^{\mu\nu} \tilde{F}_{\mu\nu}, \quad (56)$$

where g_W, g_Y, and e stand for the gauge coupling constant of $SU(2)_L$, $U(1)_Y$, and $U(1)_{EM}$, respectively, while their corresponding gauge field strengths $W^{\mu\nu}$, $Y^{\mu\nu}$, and $F^{\mu\nu}$ with their dual forms $\tilde{W}_{\mu\nu}$, $\tilde{Y}_{\mu\nu}$, and $\tilde{F}_{\mu\nu}$, respectively. Here, $N_W \equiv 2\text{Tr}[X_{\psi_f} T_{SU(2)}^2]$ and $N_Y \equiv 2\text{Tr}[X_{\psi_f} (Q_f^Y)^2]$ are the anomaly coefficients of $U(1)_X \times [SU(2)_L]^2$ and $U(1)_X \times [U(1)_Y]^2$, respectively. And the electromagnetic anomaly coefficient E of $U(1)_X \times [U(1)_{EM}]^2$ defined by $E = 2\sum_{\psi_f} X_{\psi_f} (Q_{\psi_f}^{em})^2$ with $Q_{\psi_f}^{em}$ being the $U(1)_{EM}$ charge of field ψ_f is expressed as

$$E = N_W + N_Y = -2(f_e + f_\mu + f_\tau)$$
$$- \frac{2}{3}(4f_u + 4f_c + f_d + f_s + f_b). \quad (57)$$

The physical quantities of QCD axion, such as axion mass m_a and axion-photon coupling $g_{a\gamma\gamma}$, are dependent on the ratio of electromagnetic anomaly coefficient E to color one N_C. The value of E/N_C is determined in terms of the X charges for quarks and leptons by the relation,

$$\frac{E}{N_C} = \frac{2(f_e + f_\mu + f_\tau) + \frac{2}{3}(4f_u + 4f_c + f_d + f_s + f_b)}{f_u + f_c + f_d + f_s + f_b}$$
$$= \frac{6(f_e + f_\mu + f_\tau) + 2(4f_u + 4f_c + f_d + f_s + f_b)}{-f_e - f_\mu - f_\tau - g_e - g_\mu - g_\tau}, \quad (58)$$

where the first and second equalities follow from Eqs. (52) and (54), respectively. Our model with a specific value of E/N_C can be tested by ongoing experiments such as KLASH [33] and FLASH [34] [see Eq. (76) and Figs. 1 and 2] by considering the scale of $U(1)_X$ breakdown induced by Eq. (45).

Compared to conventional A_4 symmetry models resulting in tribimaximal [36] or nearly tribimaximal [37] mixing in the neutrino sector, the modular invariant model leads to neutrino mixing without the need for special breaking patterns and the introduction of multiple scalar fields. Our model can be *uniquely* realized for quark sector by assigning $A_4 \times U(1)_X$ quantum numbers to matter fields with appropriate modular forms based on Eq. (2). Some comments are worth noting. First, by selecting the appropriate modular weight for the right-handed down-type quark fields, it is possible to construct down-type quark Yukawa superpotential with lower modular weight forms $Y_3^{(2)}$ or $Y_3^{(4)}$ while keeping the same up-type quark Yukawa superpotential given in Eq. (50). However, it is hard to reproduce the experimental data for quark masses and mixing hierarchies in this way due to the limited number of parameters. Second, unlike the case in Table I, the quark $SU(2)_L$ doublets and singlets can be assigned to A_4 triplets and singlets by choosing appropriate modular weight forms
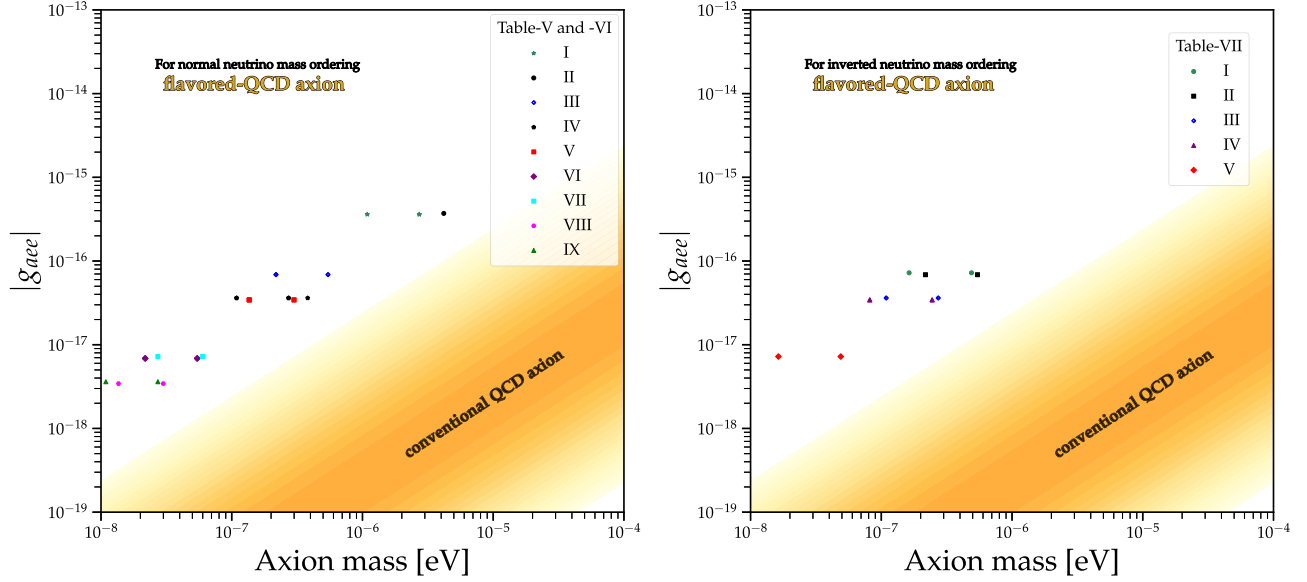
FIG. 2.   Plots for axion-electron coupling $|g_{aee}|$ as a function of the flavored-QCD axion mass m_a for NO (left) and IO (right). The orange shaded region indicates the conventional QCD axion predictions.

and $U(1)_X$ quantum numbers, respectively. In this case, the quark mass hierarchies can be realized in the limit of $\langle\tau\rangle = i\infty$ (i.e., $Y_1 \to 1$, $Y_2 \to 0$, and $Y_3 \to 0$), whereas it is hard to reproduce the CKM mixing angles since additive correction terms induced by higher weight modular forms are forbidden by the modular weight zero of $\chi(\tilde{\chi})$ fields. Third, in the opposite scenario where the quark $SU(2)_L$ doublets and singlets are assigned to A_4 singlets and triplets, respectively, it is not possible to account for the observed quark mass hierarchy due to the charge assignment of $U(1)_X$. Fourth, for leptons, unlike the case in Table II, the left-handed charged-lepton $SU(2)_L$ doublets L can be assigned to the A_4 triplet, and their $U(1)_X$ quantum numbers are taken to be $\frac{1}{2} - g_l$, whereas $SU(2)_L$ singlets (e^c, μ^c, τ^c) are assigned to the A_4 singlets $(\mathbf{1}, \mathbf{1''}, \mathbf{1'})$, and $U(1)_X$ quantum numbers are taken to be $(g_l - f_e - \frac{1}{2}, g_l - f_\mu - \frac{1}{2}, g_l - f_\tau - \frac{1}{2})$. To generate neutrino mass through the seesaw mechanism, N^c is assigned to the A_4 triplet, and the $U(1)_X$ quantum number is taken to be $-\frac{1}{2}$. In this case, we have the freedom to select the weights. For instance, we can choose the following weights: $k_L = \frac{5}{2}$, $k_{e^c} = k_{\mu^c} = k_{\tau^c} = -\frac{3}{2}$, and $k_{N^c} = \frac{1}{2}$. Then, the lepton Yukawa superpotential reads

$$W_{\ell\nu} = \left[\alpha_\tau^{(0)}\left(\frac{\mathcal{F}}{\Lambda}\right)^{|f_\tau|}(Y_3^{(2)}L)_{\mathbf{1''}}\tau^c + \alpha_\mu^{(0)}\left(\frac{\mathcal{F}}{\Lambda}\right)^{|f_\mu|}(Y_3^{(2)}L)_{\mathbf{1'}}\mu^c\right.$$
$$\left. + \alpha_e^{(0)}\left(\frac{\mathcal{F}}{\Lambda}\right)^{|f_e|}(Y_3^{(2)}L)_{\mathbf{1}}e^c\right]H_d$$
$$+ \beta^{(0)}\left(\frac{\mathcal{F}}{\Lambda}\right)^{|g_l|}(N^cL)_{\mathbf{1}}H_u + \gamma^{(0)}\frac{1}{2}(Y_3^{(2)}N^cN^c)_{\mathbf{1}}\chi + \cdots,$$

$$(59)$$

where dots stand for higher-order contributions triggered by the combination $\chi\tilde{\chi}$. It is worth noting that the above superpotential enables mixing between different charged leptons, analogous to the down-type quark sector. Additionally, the Dirac neutrino Yukawa matrix, denoted as m_D, exhibits a proportional relationship to $m_D^\dagger m_D \propto (1,1,1)$, and the heavy Majorana neutrino mass term follows a similar form, as found in Ref. [3]. By selecting other specific weights, namely, $k_L = \frac{9}{2}$, $k_{e^c} = k_{\mu^c} = k_{\tau^c} = -\frac{7}{2}$, and $k_{N^c} = -\frac{3}{2}$, a notable change occurs in the modular form of the Majorana neutrino operator. Specifically, the term $Y_3^{(2)}$ transforms into $Y_{\mathbf{1}(\mathbf{3})}^{(6)}$, resulting in an expression that aligns with the form presented in Eq. (53). While these cases show potential for reproducing lepton mass and mixing, further investigation is necessary to confirm its viability. Fifth, it is difficult to explain the mass hierarchy of the charged leptons when we assign the three right-handed charged leptons, the left-handed charged leptons and N^c to the A_4 triplet, three A_4 singlets $(\mathbf{1}, \mathbf{1''}, \mathbf{1'})$ and the A_4 triplet, respectively. This difficulty is caused by the charge assignment of $U(1)_X$.

IV. QUARK AND LEPTON INTERACTIONS WITH QCD AXION

Let us discuss how quark and lepton masses and mixings are derived from Yukawa interactions within a framework based on $A_4 \times U(1)_X$ symmetries with modular invariance. Nonzero VEVs of scalar fields $\chi(\tilde{\chi})$ spontaneously break

the flavor symmetry $U(1)_X$[10] at high energies above EW scale and create a heavy Majorana neutrino mass term. Then, the effective Yukawa structures in the low-energy limit depend on a small dimensionless parameter $\langle \mathcal{F} \rangle / \Lambda \equiv \Delta_{\mathcal{F}}$. The higher-order contributions of superpotentials $W^{(h)}_{q(l\nu)}$ become $\sum_{n=1}^{\infty} \tilde{c}_i \Delta_\chi^{2n} \cdot$ (leading-order operators) with $\tilde{c}_i = e^{i\tilde{\theta}_i}$, which make the Yukawa coefficients of the leading-order terms in the superpotentials given in Eqs. (37), (50), and (53) shifted. Denoting the effective Yukawa coefficients shifted by higher-order contributions as α_i, β_i, and γ_i, we see that they are constrained as

$$1 - \frac{\Delta_\chi^2}{1-\Delta_\chi^2} \le |\alpha_i|, \qquad |\beta_|, \qquad |\gamma_i| \le 1 + \frac{\Delta_\chi^2}{1-\Delta_\chi^2}$$

$$\text{with} \quad \Delta_\chi \equiv \frac{v_\chi}{\sqrt{2}\Lambda}, \tag{60}$$

where the lower (upper) limit corresponds to the sum of higher-order terms with $\tilde{\theta}_i = \pi(0)$. When $H_{u(d)}$ acquire nonzero VEVs, all quarks and leptons obtain masses. The relevant quark and lepton interactions with their chiral fermions are given by

$$-\mathcal{L} \supset \overline{q_R^u} \mathcal{M}_u q_L^u + \overline{q_R^d} \mathcal{M}_d q_L^d + \frac{g}{\sqrt{2}} W_\mu^+ \overline{q_L^u} \gamma^\mu q_L^d$$
$$+ \overline{\ell_R} \mathcal{M}_\ell \ell_L + \frac{1}{2} \begin{pmatrix} \overline{\nu_L^c} & \overline{N_R} \end{pmatrix} \begin{pmatrix} 0 & m_D^T \\ m_D & e^{i\frac{A_X}{u_\chi}} M_R \end{pmatrix} \begin{pmatrix} \nu_L \\ N_R^c \end{pmatrix}$$
$$+ \frac{g}{\sqrt{2}} W_\mu^- \overline{\ell_L} \gamma^\mu \nu_L + \text{H.c.}, \tag{61}$$

where g is the $SU(2)_L$ coupling constant, $q^u = (u,c,t)$, $q^d = (d,s,b)$, $\ell = (e,\mu,\tau)$, $\nu = (\nu_e, \nu_\mu, \nu_\tau)$, and $N = (N_1, N_2, N_3)$. M_R contains a VEV of χ presented by Eq. (48). The explicit forms of $\mathcal{M}_{u,d,l}$ will be given later. The above Lagrangian of the fermions, including their kinetic terms of Eq. (46), should be invariant under $U(1)_X$,

$$\psi_f \to e^{if_{\psi_f} \frac{\gamma_5}{2}\alpha} \psi_f, \quad t = \text{invariant}, \quad N \to e^{i\frac{\gamma_5}{2}\alpha} N, \tag{62}$$

where $\psi_f = \{u, c, d, s, b, e, \mu, \tau\}$ and α is a transformation constant parameter.

A. Quark and flavored-QCD axion

As axion models, the axion-Yukawa coupling matrices and quark mass matrices in our model can be simultaneously diagonalized. The quark mass matrices are diagonalized through biunitary transformations

---

$V_R^\psi \mathcal{M}_\psi V_L^{\psi\dagger} = \hat{\mathcal{M}}_\psi$ (diagonal form), and the mass eigenstates are $\psi_R' = V_R^\psi \psi_R$ and $\psi_L' = V_L^\psi \psi_L$. These transformation include, in particular, the chiral transformation of Eq. (62) that necessarily makes $\mathcal{M}_{u,d,\ell}$ real and positive. This induces a contribution to the QCD vacuum angle in Eq. (46), i.e.,

$$\vartheta_{\text{QCD}} \to \vartheta_{\text{eff}} = \vartheta_{\text{QCD}} + \arg\{\det(\mathcal{M}_u)\det(\mathcal{M}_d)\} \tag{63}$$

with $-\pi \le \vartheta_{\text{eff}} \le \pi$. Then, one obtains the vanishing QCD anomaly term

$$\mathcal{L}_\vartheta = \left(\vartheta_{\text{eff}} + \frac{A_X}{F_a} \right) \frac{\alpha_s'}{8\pi} G^{a\mu\nu} \tilde{G}^a_{\mu\nu} \quad \text{with} \quad F_a = \frac{f_a}{N_C}, \tag{64}$$

where $\alpha_s' = g_s^2/4\pi$ and the axion decay constant F_a with $f_a = u_\chi$ of Eq. (48). At low energies, A_X will get a VEV, $\langle A_X \rangle = -F_a \vartheta_{\text{eff}}$, eliminating the constant ϑ_{eff} term. The QCD axion then is the excitation of the A_X field, $a = A_X - \langle A_X \rangle$.

Substituting the VEV of Eq. (40) into the superpotential (50), the mass matrices $\mathcal{M}_u$ and $\mathcal{M}_d$ for up- and down-type quarks given in the Lagrangian (61) are derived as

$$\mathcal{M}_u = \begin{pmatrix} \alpha_u \Delta_\chi^{|f_u|} Y_1^{(6)} e^{if_u \frac{A_X}{u_\chi}} & 0 & 0 \\ 0 & \alpha_c \Delta_\chi^{|f_c|} Y_1^{(6)} e^{if_c \frac{A_X}{u_\chi}} & 0 \\ 0 & 0 & \alpha_t \end{pmatrix} v_u, \tag{65}$$

$$\mathcal{M}_d = \left[\begin{pmatrix} \alpha_d \Delta_\chi^{|f_d|} & \alpha_s x \Delta_\chi^{|f_s|} & \alpha_b y \Delta_\chi^{|f_b|} \\ \alpha_d y \Delta_\chi^{|f_d|} & \alpha_s \Delta_\chi^{|f_s|} & \alpha_b x \Delta_\chi^{|f_b|} \\ \alpha_d x \Delta_\chi^{|f_d|} & \alpha_s y \Delta_\chi^{|f_s|} & \alpha_b \Delta_\chi^{|f_b|} \end{pmatrix} (1+2xy) \right.$$
$$+ \left. \begin{pmatrix} \tilde{\alpha}_d y \Delta_\chi^{|f_d|} & \tilde{\alpha}_s \Delta_\chi^{|f_s|} & \tilde{\alpha}_b x \Delta_\chi^{|f_b|} \\ \tilde{\alpha}_d x \Delta_\chi^{|f_d|} & \tilde{\alpha}_s y \Delta_\chi^{|f_s|} & \tilde{\alpha}_b \Delta_\chi^{|f_b|} \\ \tilde{\alpha}_d \Delta_\chi^{|f_d|} & \tilde{\alpha}_s x \Delta_\chi^{|f_s|} & \tilde{\alpha}_b y \Delta_\chi^{|f_b|} \end{pmatrix} (y^2 + 2x) \right] \tilde{C} Y_1^3 v_d, \tag{66}$$

where $v_d \equiv \langle H_d \rangle = v \cos\beta/\sqrt{2}$, $v_u \equiv \langle H_u \rangle = v \sin\beta/\sqrt{2}$ with $v \simeq 246$ GeV, and

$$\tilde{C} = \text{diag}\left(e^{if_d \frac{A_X}{u_\chi}}, e^{if_s \frac{A_X}{u_\chi}}, e^{if_b \frac{A_X}{u_\chi}} \right), \quad x = \frac{Y_2}{Y_1}, \quad y = \frac{Y_3}{Y_1}. \tag{67}$$

The terms with $\alpha_{d,s,b}$ in Eq. (66) generate by taking the modular form $Y_{3,1}^{(6)}$ given in Eq. (51), whereas the terms with $\tilde{\alpha}_{d,s,b}$ in Eq. (66) generate by taking $Y_{3,2}^{(6)}$.

The quark mass matrices $\mathcal{M}_u$ in Eq. (65) and $\mathcal{M}_d$ in Eq. (66) generate the up- and down-type quark masses:

$$\hat{\mathcal{M}}_u = V_R^u \mathcal{M}_u V_L^{u\dagger} = \text{diag}(m_u, m_c, m_t),$$
$$\hat{\mathcal{M}}_d = V_R^d \mathcal{M}_d V_L^{d\dagger} = \text{diag}(m_d, m_s, m_b). \tag{68}$$

Diagonalizing the matrices $\mathcal{M}_f^\dagger \mathcal{M}_f$ and $\mathcal{M}_f \mathcal{M}_f^\dagger$ ($f = u, d$) determines the mixing matrices V_L^f and V_R^f, respectively [38]. The left-handed quark mixing matrices V_L^u and V_L^d are components of the CKM matrix $V_{\text{CKM}} = V_L^u V_L^{d\dagger}$, which is generated from the down-type quark matrix in Eq. (66) due to the diagonal form of the up-type quark mass matrix in Eq. (65). The CKM matrix is parametrized by the Wolfenstein parametrization [39] [see Eq. (B1)] and has been determined with high precision [40]. The current best-fit values of the CKM mixing angles in the standard parametrization [41] read in the 3σ range [42]

$$\theta_{23}^q[^\circ] = 2.376^{+0.054}_{-0.070}, \qquad \theta_{13}^q[^\circ] = 0.210^{+0.016}_{-0.010},$$
$$\theta_{12}^q[^\circ] = 13.003^{+0.048}_{-0.036}, \qquad \delta_{CP}^q[^\circ] = 65.5^{+3.1}_{-4.9}. \tag{69}$$

The physical structure of the up- and down-type quark Lagrangian should match up with the empirical results calculated from the Particle Data Group (PDG) [35],

$$m_d = 4.67^{+0.48}_{-0.17} \text{ MeV}, \qquad m_s = 93^{+11}_{-5} \text{ MeV},$$
$$m_b = 4.18^{+0.03}_{-0.02} \text{ GeV}, \qquad m_u = 2.16^{+0.49}_{-0.29} \text{ MeV},$$
$$m_c = 1.27 \pm 0.02 \text{ GeV}, \qquad m_t = 173.1 \pm 0.9 \text{ GeV}, \tag{70}$$

where t-quark mass is the pole mass; c- and b-quark masses are the running masses in the $\overline{\text{MS}}$ scheme; and the light u-, d-, and s-quark masses are the current quark masses in the $\overline{\text{MS}}$ scheme at the momentum scale $\mu \approx 2$ GeV. Below the scale of spontaneous $SU(2)_L \times U(1)_Y$ gauge symmetry breaking, the running masses of c and b quarks receive corrections from QCD and QED loops [35]. The top-quark mass at scales below the pole mass is unphysical since the t-quark decouples at its scale, and its mass is determined more directly by experiments [35].

After diagonalizing the mass matrices of Eqs. (65) and (66), the flavored-QCD axion to quark interactions are written at leading order as

$$\begin{aligned}
-\mathcal{L}^{aq} \simeq &\, \frac{\partial_\mu a}{2u_\chi} \{ f_u \bar{u} \gamma^\mu \gamma_5 u + f_c \bar{c} \gamma^\mu \gamma_5 c + f_d \bar{d} \gamma^\mu \gamma_5 d + f_s \bar{s} \gamma^\mu \gamma_5 s + f_b \bar{b} \gamma^\mu \gamma_5 b \} \\
&+ \frac{\partial_\mu a}{2u_\chi} \left\{ (f_d - f_s) \lambda \left(1 - \frac{\lambda^2}{2} \right) \bar{d} \gamma^\mu \gamma_5 s + (f_s - f_b) A_d \lambda^2 \bar{s} \gamma^\mu \gamma_5 b \right. \\
&+ A_d \lambda^3 (f_d(\rho + i\eta) - f_s + f_b(1 - \rho - i\eta)) \bar{b} \gamma^\mu \gamma_5 d + \text{H.c.} \bigg\} \\
&+ i \frac{a}{2u_\chi} \left\{ (f_d - f_s) \lambda \left(1 - \frac{\lambda^2}{2} \right) (m_d - m_s) \bar{d} s + (f_s - f_b) A_d \lambda^2 (m_s - m_b) \bar{s} b \right. \\
&+ A_d \lambda^3 (f_d(\rho + i\eta) - f_s + f_b(1 - \rho - i\eta))(m_b - m_d) \bar{b} d + \text{H.c.} \bigg\} \\
&+ m_u \bar{u} u + m_c \bar{c} c + m_t \bar{t} t + m_d \bar{d} d + m_s \bar{s} s + m_b \bar{b} b - \bar{q} i \slashed{D} q,
\end{aligned} \tag{71}$$

where $V_L^{d\dagger} = V_{\text{CKM}}$ of Eq. (B1) is used by rotating the phases in $\mathcal{M}_u$ away, which is the result of a direct interaction of the SM gauge singlet scalar field χ with the SM quarks charged under $U(1)_X$. The flavored-QCD axion a is produced by flavor-changing neutral Yukawa interactions in Eq. (71), which leads to induced rare flavor-changing processes. The strongest bound on the QCD axion decay constant is from the flavor-changing process $K^+ \to \pi^+ + a$ [43–47], induced by the flavored-QCD axion a. From Eq. (71), the flavored-QCD axion interactions with the flavor-violating coupling to the s and d quarks are given by

$$-\mathcal{L}_Y^{asd} \simeq \frac{i}{2}(f_d - f_s) \frac{a}{N_C F_a} \bar{s} d(m_d - m_s) \lambda \left(1 - \frac{\lambda^2}{2} \right). \tag{72}$$

Then, the decay width of $K^+ \to \pi^+ + a$ is given by

$$\Gamma(K^+ \to \pi^+ + a) = \frac{m_K^3}{16\pi} \left(1 - \frac{m_\pi^2}{m_K^2} \right)^3 \left| \frac{f_d - f_s}{2F_a N_C} \lambda \left(1 - \frac{\lambda^2}{2} \right) \right|^2, \tag{73}$$

where $m_{K^\pm} = 493.677 \pm 0.013$ MeV, $m_{\pi^\pm} = 139.57061 \pm 0.00024$ MeV [35]. From the present experimental upper bound $\text{Br}(K^+ \to \pi^+ a) < (3 - 6) \times 10^{-11}(1 \times 10^{-11})$ for $m_a = 0$–110 (160–260) MeV at 90% C.L. with $\text{Br}(K^+ \to \pi^+ \nu \bar{\nu}) = (10.6^{+4.0}_{-3.4}|_{\text{stat}} \pm 0.9_{\text{syst}}) \times 10^{-11}$ at 68% C.L. [48], we obtain the lower limit on the QCD axion decay constant,

$$F_a \frac{2|N_C|}{|f_d - f_s|} \gtrsim (0.86 - 1.90) \times 10^{11} \text{ GeV}. \quad (74)$$

The QCD axion mass m_a in terms of the pion mass and pion decay constant reads [17,18]

$$m_a^2 F_a^2 = m_{\pi^0}^2 f_\pi^2 F(z, w), \quad (75)$$

where $f_\pi \simeq 92.1$ MeV [35] and $F(z, w) = z/(1 + z)(1 + z + w)$ with $\omega = 0.315z$. Here, the Weinberg value lies in $z \equiv m_u^{\overline{\text{MS}}}(2 \text{ GeV})/m_d^{\overline{\text{MS}}}(2 \text{ GeV}) = 0.47^{+0.06}_{-0.07}$ [35]. After integrating out the heavy π^0 and η at low energies, there is an effective low-energy Lagrangian with an axion-photon coupling $g_{a\gamma\gamma}$: $\mathcal{L}_{a\gamma\gamma} = -g_{a\gamma\gamma} a\vec{E} \cdot \vec{B}$ where $\vec{E}$ and $\vec{B}$ are the electromagnetic field components. The axion coupling is expressed as,

$$g_{a\gamma\gamma} = \frac{\alpha_{\text{em}}}{2\pi} \frac{m_a}{f_\pi m_{\pi^0}} \frac{1}{\sqrt{F(z, w)}} \left(\frac{E}{N_C} - \frac{2}{3} \frac{4 + z + w}{1 + z + w} \right). \quad (76)$$

The upper bound on the axion-photon coupling, derived from the recent analysis of the horizontal branch stars in galactic globular clusters [49], can be translated to

$$|g_{a\gamma\gamma}| < 6.6 \times 10^{-11} \text{ GeV}^{-1}(95\% \text{ CL})$$

$$\Leftrightarrow F_a \gtrsim 2.525 \times 10^7 \left| \frac{E}{N_C} - 1.903 \right| \text{ GeV}, \quad (77)$$

where $z = 0.47$ is used.

B. Charged-lepton and flavored-QCD axion

Substituting the VEV of Eq. (40) into the superpotential (53), the charged-lepton mass matrix given in the Lagrangian (61) is derived as

$$\mathcal{M}_\ell = \begin{pmatrix} \alpha_e \Delta_\chi^{|f_e|} e^{if_e \frac{A_X}{u_\chi}} & 0 & 0 \\ 0 & \alpha_\mu \Delta_\chi^{|f_\mu|} e^{if_\mu \frac{A_X}{u_\chi}} & 0 \\ 0 & 0 & \alpha_\tau \Delta_\chi^{|f_\tau|} e^{if_\tau \frac{A_X}{u_\chi}} \end{pmatrix} Y_1^{(6)} v_d. \quad (78)$$

Recall that the coefficients α_i are complex numbers with an effective absolute value satisfying Eq. (60). Then, the corresponding charged-lepton masses are given by

$$m_e = \alpha_e Y_1^{(6)} \Delta_\chi^{|f_e|} v_d, \qquad m_\mu = \alpha_\mu Y_1^{(6)} \Delta_\chi^{|f_\mu|} v_d,$$

$$m_\tau = \alpha_\tau Y_1^{(6)} \Delta_\chi^{|f_\tau|} v_d, \quad (79)$$

where $Y_1^{(6)}$ is given in Eq. (51) and the phases in each term can be absorbed into $(l_i)_R$. They are matched with the empirical values from the PDG [35] given by

$$m_e = 0.511 \text{ MeV}, \qquad m_\mu = 105.658 \text{ MeV},$$

$$m_\tau = 1776.86 \pm 0.12 \text{ MeV}. \quad (80)$$

Flavored axions typically interact with charged leptons (electrons, muons, and taus) [17,18,20,21] and can be emitted through atomic axiorecombination, axiodeexcitation, axiobremsstrahlung in electron-ion or electron-electron collisions, and Compton scatterings [50]. Then, the flavored-QCD axion to charged-lepton interactions read

$$-\mathcal{L}^{a\ell} \simeq \frac{\partial_\mu a}{2u_\chi} (f_e \bar{e}\gamma^\mu\gamma_5 e + f_\mu \bar{\mu}\gamma^\mu\gamma_5 \mu + f_\tau \bar{\tau}\gamma^\mu\gamma_5 \tau)$$

$$+ \sum_{\ell=e,\mu,\tau} (m_\ell \bar{\ell}\ell - \bar{\ell}i\partial\!\!\!/\ell). \quad (81)$$

Like rare neutral flavor-changing decays in particle physics, the interaction of the flavored-QCD axion a with leptons makes it possible to search for the QCD axion in astroparticle physics through stellar evolution. The flavored-QCD axion coupling to electrons reads

$$g_{aee} = |f_e| \frac{m_e}{u_\chi}. \quad (82)$$

Stars in the red giant branch of color-magnitude diagrams in globular clusters provide a strict constraint on axion-electron couplings, which leads to a lower bound on the axion decay constant. This constraint is expressed as [51]

$$|g_{aee}| < 4.3 \times 10^{-13}(95\% \text{ C.L.})$$

$$\Leftrightarrow N_C F_a \gtrsim 1.19|f_e| \times 10^9 \text{ GeV}. \quad (83)$$

Bremsstrahlung off electrons $e + Ze \rightarrow Ze + e + a$ in white dwarfs (WDs) is an effective process for detecting axions, as the Primakoff and Compton processes are suppressed due to the large plasma frequency. Comparing the theoretical and observed WD luminosity functions (WDLFs) provides a way to place limits[11] on $|g_{aee}|$ [56]. Recent analyses of WDLFs, using detailed WD cooling treatment and new data on the WDLF of the Galactic disk, suggest electron couplings $|g_{aee}| \lesssim 2.8 \times 10^{-13}$ [52]. However, these results come with large theoretical and observational uncertainties.

We note that the entries of the quark and charged-lepton mass matrices given in Eqs. (65), (66), and (78) except for

---

[11]Note that Refs. [52,53] have pointed out features in some WDLFs [54,55] that could imply axion-electron couplings in the range $7.2 \times 10^{-14} \lesssim |g_{aee}| \lesssim 2.2 \times 10^{-13}$.

the entry corresponding to the top quark are expressed as a combination of $\Delta_\chi^{|f_\alpha|}$ and modular forms for each component. Accurate determination of the values of Δ_χ, its power, and the value of τ is crucial to reproduce the observed CKM mixing angles given in Eq. (69) and quark masses in Eq. (70). The values of those parameters are also closely linked to those in the lepton sector, and they should necessarily be determined in order to reproduce the observed values of charged-lepton masses and to predict

light active neutrinos derived from Eqs. (84) and (86). The $U(1)_X$ PQ scale, which corresponds to the seesaw scale [as shown n Eq. (85)], can be estimated as $\mu_\chi \sim 6 \times 10^{13}$ GeV from Eq. (45) for $m_{3/2} \sim 100$ TeV.

C. Neutrino

Similar to the case of charged-lepton mass matrix, the heavy Majorana mass matrix given in the Lagrangian (61) is derived from the superpotential (53) as

$$
M_R = M \begin{pmatrix} 1 + y^3 - 5xy & 0 & 0 \\ 0 & 0 & 1 + y^3 - 5xy \\ 0 & 1 + y^3 - 5xy & 0 \end{pmatrix}
$$
$$
+ M \begin{pmatrix} \frac{2}{\sqrt{3}}(\gamma p + \gamma' yr) & -\frac{1}{\sqrt{3}}(\gamma yp + \gamma' xr) & -\frac{1}{\sqrt{3}}(\gamma xp + \gamma' r) \\ -\frac{1}{\sqrt{3}}(\gamma yp + \gamma' xr) & \frac{2}{\sqrt{3}}(\gamma xp + \gamma' r) & -\frac{1}{\sqrt{3}}(\gamma p + \gamma' yr) \\ -\frac{1}{\sqrt{3}}(\gamma xp + \gamma' r) & -\frac{1}{\sqrt{3}}(\gamma p + \gamma' yr) & \frac{2}{\sqrt{3}}(\gamma yp + \gamma' xr) \end{pmatrix}, \tag{84}
$$

where $p = 1 + 2xy$, $r = y^2 + 2xy$, $\gamma = \gamma_2/\gamma_1$, $\gamma' = \gamma_2'/\gamma_1$, and the common factor M can be replaced by the QCD axion decay constant F_a,

$$
M \equiv |\gamma_1 Y_1^3 \langle \chi \rangle| = \frac{|\gamma_1|}{2} F_a |N_C Y_1^3|. \tag{85}
$$

The terms with γ_2 in Eq. (84) are derived by taking the modular form $Y_{3,1}^{(6)}$ satisfying Eq. (51), whereas the terms with γ_2' are derived by taking $Y_{3,2}^{(6)}$. Equation (84) has three unknown complex parameters, γ, γ', and γ_1, where the phase of γ_1 contributes as an overall factor after seesawing. Other variables such as x, y, and Y_1 are determined from the analysis for the quark and charged-lepton sectors, and $\langle \chi \rangle$ is fixed from the seesaw formula (87) whose scale is given by PQ scale (45). The Dirac mass term in the Lagrangian (61) reads

$$
m_D = \begin{pmatrix} \beta_1 \Delta_\chi^{|g_e|} & \beta_2 y \Delta_\chi^{|g_\mu|} & \beta_3 x \Delta_\chi^{|g_\tau|} \\ \beta_1 y \Delta_\chi^{|g_e|} & \beta_2 x \Delta_\chi^{|g_\mu|} & \beta_3 \Delta_\chi^{|g_\tau|} \\ \beta_1 x \Delta_\chi^{|g_e|} & \beta_2 \Delta_\chi^{|g_\mu|} & \beta_3 y \Delta_\chi^{|g_\tau|} \end{pmatrix}
$$
$$
\times \begin{pmatrix} e^{ig_e \frac{A_X}{u_\chi}} & 0 & 0 \\ 0 & e^{ig_\mu \frac{A_X}{u_\chi}} & 0 \\ 0 & 0 & e^{ig_\tau \frac{A_X}{u_\chi}} \end{pmatrix} Y_1 v_u. \tag{86}
$$

The coefficients β_i and γ_i in the neutrino sector, like in the quark and charged-lepton sectors, are complex numbers corrected by higher-dimensional operators, resulting in an effective absolute value satisfying Eq. (60). Equation (86) contains three complex parameters (β_1, β_2, and β_3), where one of the phases can be removable as an overall factor after seesawing. As shown before, the parameter Δ_χ can be determined from quark and charged-lepton sectors. In addition, its $U(1)_X$ quantum number g_α can be determined from the numerical analysis for the neutrino sector with the help of the condition of $U(1)_X$-mixed gravitational anomaly free given in Eq. (54).

After integrating out the right-handed heavy Majorana neutrinos, the effective neutrino mass matrix $\mathcal{M}_\nu$ is given at leading order by

$$
\mathcal{M}_\nu \simeq -m_D^T M_R^{-1} m_D = U_\nu^* \text{diag}(m_{\nu_1}, m_{\nu_2}, m_{\nu_3}) U_\nu^\dagger, \tag{87}
$$

where U_ν is the rotation matrix diagonalizing $\mathcal{M}_\nu$ and m_{ν_i} ($i = 1, 2, 3$) are the light neutrino masses. Then, the PMNS mixing matrix becomes

$$
U_{\text{PMNS}} = U_\nu. \tag{88}
$$

The matrix U_{PMNS} is expressed in terms of three mixing angles, θ_{12}, θ_{13}, θ_{23}, and a Dirac-type CP-violating phase δ_{CP} and two additional CP-violating phases $\varphi_{1,2}$ if light neutrinos are Majorana particles as [35]

TABLE III.   The global fit of three-flavor oscillation parameters at the best-fit and 3σ level with Super-Kamiokande atmospheric data [61]. $\Delta m^2_{\mathrm{Sol}} \equiv m^2_{\nu_2} - m^2_{\nu_1}$, $\Delta m^2_{\mathrm{Atm}} \equiv m^2_{\nu_3} - m^2_{\nu_1}$ for NO, and $\Delta m^2_{\mathrm{Atm}} \equiv m^2_{\nu_2} - m^2_{\nu_3}$ for IO.

	$\theta_{13}(°)$	$\delta_{CP}(°)$	$\theta_{12}(°)$	$\theta_{23}(°)$	$\Delta m^2_{\mathrm{Sol}}(10^{-5}\ \mathrm{eV}^2)$	$\Delta m^2_{\mathrm{Atm}}(10^{-3}\ \mathrm{eV}^2)$
NO	$8.58^{+0.33}_{-0.35}$	232^{+118}_{-88}	$33.41^{+2.33}_{-2.10}$	$42.2^{+8.8}_{-2.5}$	$7.41^{+0.62}_{-0.59}$	$2.507^{+0.083}_{-0.080}$
IO	$8.57^{+0.37}_{-0.34}$	276^{+68}_{-82}		$49.0^{+2.5}_{-9.1}$		$2.486^{+0.084}_{-0.080}$

$$U_{\mathrm{PMNS}} = \begin{pmatrix} c_{13}c_{12} & c_{13}s_{12} & s_{13}e^{-i\delta_{CP}} \\ -c_{23}s_{12} - s_{23}c_{12}s_{13}e^{i\delta_{CP}} & c_{23}c_{12} - s_{23}s_{12}s_{13}e^{i\delta_{CP}} & s_{23}c_{13} \\ s_{23}s_{12} - c_{23}c_{12}s_{13}e^{i\delta_{CP}} & -s_{23}c_{12} - c_{23}s_{12}s_{13}e^{i\delta_{CP}} & c_{23}c_{13} \end{pmatrix} Q_\nu, \tag{89}$$

where $s_{ij} \equiv \sin\theta_{ij}$, $c_{ij} \equiv \cos\theta_{ij}$ and $Q_\nu = \mathrm{Diag}(e^{-i\varphi_1/2}, e^{-i\varphi_2/2}, 1)$. Then, the neutrino masses are obtained by the transformation

$$U^T_{\mathrm{PMNS}} \mathcal{M}_\nu U_{\mathrm{PMNS}} = \mathrm{Diag}(m_{\nu_1}, m_{\nu_2}, m_{\nu_3}). \tag{90}$$

Here, m_{ν_i} ($i = 1, 2, 3$) are the light neutrino masses. The observed hierarchy $|\Delta m^2_{\mathrm{Atm}}| = |m^2_{\nu_3} - (m^2_{\nu_1} + m^2_{\nu_2})/2| \gg \Delta m^2_{\mathrm{Sol}} \equiv m^2_{\nu_2} - m^2_{\nu_1} > 0$ and the requirement of a Mikheyev-Smirnov-Wolfenstein resonance [57] for solar neutrinos lead to two possible neutrino mass spectra: normal mass ordering (NO) $m^2_{\nu_1} < m^2_{\nu_2} < m^2_{\nu_3}$ and inverted mass ordering (IO) $m^2_{\nu_3} < m^2_{\nu_1} < m^2_{\nu_2}$. Nine physical observables can be derived from Eqs. (89) and (90): θ_{23}, θ_{13}, θ_{12}, δ_{CP}, φ_1, φ_2, m_{ν_1}, m_{ν_2}, and m_{ν_3}. Recent global fits [58–60] of neutrino oscillations have enabled a more precise determination of the mixing angles and mass squared differences, with large uncertainties remaining for θ_{23} and δ_{CP} at 3σ. The most recent analysis [61] lists global fit values and 3σ intervals for these parameters in Table III. Furthermore, recent constraints on the rate of $0\nu\beta\beta$ decay have added to these findings. Specifically, the tightest upper bounds for the effective Majorana mass $(\mathcal{M}_\nu)_{ee}$, which is the modulus of the ee entry of the effective neutrino mass matrix, are given by

$$(\mathcal{M}_\nu)_{ee} < 0.036 - 0.156\,\mathrm{eV} \quad (^{136}\mathrm{Xe\text{-}based\ experiment}\,[62]) \tag{91}$$

at 90% confidence level. $0\nu\beta\beta$ decay is a low-energy probe of lepton-number violation, and its measurement could provide the strongest evidence for lepton-number violation at high energy. Its discovery would suggest the Majorana nature of neutrinos and, consequently, the existence of heavy Majorana neutrinos via the seesaw mechanism [1].

Transforming the neutrino fields by chiral rotations of Eq. (62) under $U(1)_X$, we obtain the flavored-QCD axion interactions to neutrinos

$$-\mathcal{L}^{a\nu} \simeq \frac{a}{2u_\chi} \sum_{i \neq j} \overline{\nu_i} \{ (m_{\nu_i} - m_{\nu_j})\mathrm{Im}[V]_{ij} $$
$$- i\gamma_5(m_{\nu_i} + m_{\nu_j})\mathrm{Re}[V]_{ij} \} \nu_j + \frac{\partial a}{4u_\chi} \overline{N} \gamma_\mu \gamma_5 N^c, \tag{92}$$

where m_{ν_i} are real and positive, $\mathcal{Q}[V]_{ij} = (g_e - \frac{1}{2}) \mathcal{Q}[U_{1i}U^*_{1j}] + (g_\mu - \frac{1}{2})\mathcal{Q}[U_{2i}U^*_{2j}] + (g_\tau - \frac{1}{2})\mathcal{Q}[U_{3i}U^*_{3j}]$ with $\mathcal{Q} = \mathrm{Re}$ or Im, and $\mathrm{Im}[V]_{ij} = -\mathrm{Im}[V]_{ji}$ with $U \equiv U_{\mathrm{PMNS}}$. Since the light neutrino mass is less than 0.1 eV, the coupling between the flavored-QCD axion and light neutrinos is subject to a stringent constraint given by Eq. (74), which significantly suppresses the interaction. Therefore, we will not take it into consideration. Reference [62] provides the latest experimental constraints on Majoron-neutrino coupling, which are below the range of $(0.4 - 0.9) \times 10^{-5}$.

Once the lepton $U(1)_X$ quantum numbers are fixed, the seesaw scale $M \sim v_\chi$ of Eq. (85) comparable to the PQ scale of Eq. (45) can be roughly determined using the seesaw formula (87). By putting Eqs. (84) and (86) into the seesaw formula (87), we obtain numerically a range of values for $\langle \chi \rangle$. For instance, see Table IV; it implies that for normal mass ordering the maximum scale should be below $\sim 10^{15}$ GeV and for inverted mass ordering the maximum scale should be below $\sim 5 \times 10^{14}$ GeV. Refer to Tables V and VI for NO and Table VII for IO, with $F_a = 2|\langle \chi \rangle / N_C|$. By using the seesaw formula (87), one can set the scale $\langle \chi \rangle$

TABLE IV. $U(1)_X$ charges linked to seesaw scale.

	$|g_e|$	$|g_\mu|$	$|g_\tau|$	$\langle \chi \rangle/\mathrm{GeV}$
NO	6	4	5	10^{13}
	5	3	4	5×10^{13}
	4	2	3	10^{14}
	3	1	2	5×10^{14}
	2	0	1	10^{15}
IO	2	3	3	5×10^{13}
	1	2	2	10^{14}
	0	1	1	5×10^{14}

along with the $U(1)_X$ quantum numbers g_α without loss of generality. Doing so results in an effective mass matrix with nine physical degrees of freedom,

$$m_0 \equiv \left| \frac{\beta_1^2}{\gamma_1 Y_1} \right| \frac{v_u^2}{\langle \chi \rangle}, \quad |\gamma|, \quad |\gamma'|, \quad |\tilde{\beta}_2|, \quad |\tilde{\beta}_3|, \quad \arg(\gamma),$$
$$\times \arg(\gamma'), \quad \arg(\tilde{\beta}_2), \quad \arg(\tilde{\beta}_3), \quad (93)$$

in which m_0 is an overall factor of Eq. (87), $\tilde{\beta}_2 \equiv \beta_2/\beta_1, \tilde{\beta}_3 \equiv \beta_3/\beta_1$, and $1 - 2\Delta_\chi^2 \leq |\tilde{\beta}_{2(3)}|, |\gamma|, |\gamma'| \leq \frac{1}{1-2\Delta_\chi^2}$. Out of the nine observables corresponding to Eq. (93), the five measured quantities ($\theta_{12}, \theta_{23}, \theta_{13}, \Delta m_{\text{Sol}}^2, \Delta m_{\text{Atm}}^2$) can be used as constraints. The remaining four degrees of freedom correspond to four measurable quantities (δ_{CP}, $\varphi_{1,2}$, and the $0\nu\beta\beta$-decay rate), which can be determined through measurements.

V. NUMERICAL ANALYSIS FOR QUARK, LEPTON, AND A QCD AXION

To simulate and match experimental results for quarks and leptons [Eqs. (69) and (70) and Table III], we use linear algebra tools from Ref. [63]. By analyzing experimental data for quarks and charged leptons, we determined the $U(1)_X$ quantum numbers listed in Tables V and VI for normal neutrino mass ordering and Table VII for inverted neutrino mass ordering. We also ensured the $U(1)_X$-mixed gravitational anomaly-free condition of Eq. (54) and consistency of the seesaw scale discussed above Eq. (93) with the PQ-breaking scale of Eq. (45).

Notably, in our model, the flavored-QCD axion mass (and its associated PQ-breaking or seesaw scale) is closely linked to the soft SUSY-breaking mass. Our analysis covers the PQ scale $\langle \chi \rangle$ from roughly 10^{13} to 10^{15} GeV due to Table IV, corresponding to $m_{3/2}$ values of 1 to 10^6 TeV, by considering Eq. (45) and Table IV. The given $U(1)_X$ quantum numbers can then be used to predict the branching ratio of $K^+ \to \pi^+ + a$ [Eq. (73)] as well as the axion coupling to photon [Eq. (76)] and electron [Eq. (82)]. See Tables V, VI, and VII for more details. The predictions of our proposed model can be tested by current axion search experiments. KLASH [33] is sensitive to the mass range of $0.27 - 0.93 \, \mu\text{eV}$, whereas FLASH [34] covers the mass range of $0.5 - 1.5 \, \mu\text{eV}$. The predictions corresponding to those range of m_a covered by those experiments will be tested in foreseeable future. Figure 1 illustrates plots of the axion-photon coupling $|g_{a\gamma\gamma}|$ as a function of the flavored-QCD axion mass m_a for NO (left) and IO (right), respectively. Each plotted point corresponds to values listed in Tables V–VII, which are consistent with the experimental constraints described in Eqs. (74), (77), and (83). And Fig. 1 illustrates that certain data points in Table V (I-c, I-d, I-e) have been fully excluded by the ADMX experiment [64], while another data point (II) in Table V has been marginally

excluded by the same experiment. Figure 2 shows plots for axion-electron coupling $|g_{aee}|$ as a function of the flavored-QCD axion mass m_a for NO (left) and IO (right).

A. Quark and charged-lepton

The Yukawa matrices for charged fermions in the SM, as given in Eqs. (65), (66), and (78), are taken at the scale of $U(1)_X$ symmetry breakdown. Hence, their masses are subject to quantum corrections. Subsequently, these matrices are run down to m_t and diagonalized. We assume that the Yukawa matrices at the scale of $U(1)_X$ breakdown are the same as those at the scale m_t, since the one-loop renormalization group running effect on observables for hierarchical mass spectra is expected to be negligible. The low-energy Yukawa couplings required for experimental values are obtained from the physical masses and mixing angles compiled by the PDG [35] and CKMfitter [42].

We have 13 physical observables in the quark and charged-lepton sector: $m_d, m_s, m_b, m_u, m_c, m_t, m_e, m_\mu, m_\tau$, and $\theta_{12}^q, \theta_{23}^q, \theta_{13}^q, \delta_{CP}^q$. These observables are used to determine 13 effective model parameters: 21 parameters ($|\alpha_d|, |\alpha_s|, |\alpha_b|, |\tilde{\alpha}_d|, |\tilde{\alpha}_s|, |\tilde{\alpha}_b|, \alpha_e, \alpha_\mu, \alpha_\tau, \alpha_t, \alpha_c, \alpha_u$; $\arg(\alpha_d), \arg(\alpha_s), \arg(\tilde{\alpha}_d), \arg(\tilde{\alpha}_s), \arg(\tilde{\alpha}_b)$; Δ_χ, $\tan\beta$; $\text{Re}[\tau], \text{Im}[\tau]$) among which eight parameters are fixed by quantum numbers ($f_{e,\mu,\tau}, f_{d,s,b}, f_{u,c}$). Using highly precise data as constraints for both quarks and charged leptons, with the exception of the quark Dirac CP phase, as described in Eqs. (69), (70), and (80), we scanned all parameter ranges and determined that

$$\Delta_\chi = [0.596, 0.602], \qquad \tan\beta = [6.8, 7.3],$$
$$\tau = (0.0001 \sim 0.046) + (1.0906 \sim 1.1086)i. \quad (94)$$

The real part of τ, denoted as $\text{Re}(\tau)$, contributes to the phase of the Yukawa coupling, while the imaginary part of τ, denoted as $\text{Im}(\tau)$, influences the magnitude of Yukawa coupling, as demonstrated in Eqs. (65), (66), (78), (85), and (86). When $\langle \tau \rangle = i$, resulting in real values of x and y in Eq. (67) as $Y_3^{(2)} = Y_1(i)(1, 1 - \sqrt{3}, -2 + \sqrt{3})$, it becomes apparent that it is challenging to satisfy the empirical results of quark masses and CKM mixing angles due to the overall factors in Eq. (66) being real. Therefore, it is imperative to deviate τ from i in order to accommodate the phase in CKM matrix. Figure 3 shows how the quark Dirac CP phase δ_{CP}^q behaves based on certain constrained parameters. Our model predicts that δ_{CP}^q falls between 38° and 87°, which aligns well with experimental data. The horizontal black-dotted lines in Fig. 3 represent the 3σ experimental bound for δ_{CP}^q. Notably, the effective Yukawa coefficients satisfying the experimental data fall well within the bound specified in Eq. (60), as shown in the top-left panel of Fig. 3. This reflects that these coefficients have a natural size of unity, as stated in Eq. (2).
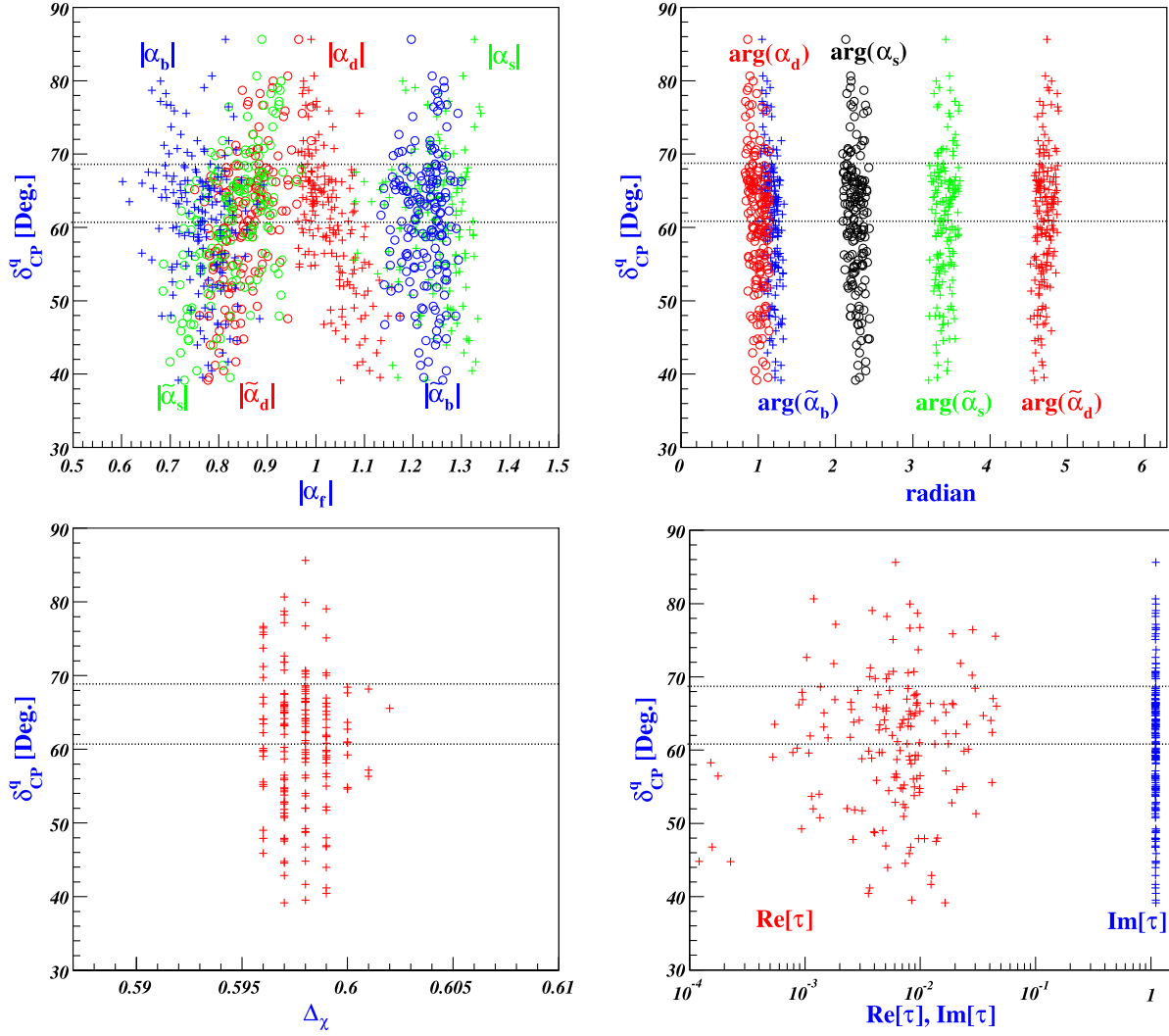
FIG. 3.   Model predictions for δ^q_{CP} are shown, left-upper, right-upper, and left-lower panels, as functions of the parameters that are constrained by other empirical results. The horizontal black-dotted lines indicate the 3σ experimental bound.

We choose reference values, for example, that satisfy the experimental data,

$$\Delta_\chi = 0.597, \qquad \tau = 0.0074 + 1.0997i, \qquad \tan\beta = 6.8, \tag{95}$$

which result in effective Yukawa coefficients from Eq. (60) satisfying $0.45 \lesssim |\alpha_i| \lesssim 1.55$. With the inputs

$$\arg(\alpha_d) = 1.007, \quad \arg(\alpha_s) = 2.232, \quad \arg(\tilde{\alpha}_d) = 4.723, \quad \arg(\tilde{\alpha}_s) = 3.388, \quad \arg(\tilde{\alpha}_b) = 1.164,$$

$$\alpha_u = 1.320 \quad \text{for } |f_u| = 21 (\alpha_u = 0.788 \quad \text{for } |f_u| = 20), \quad \alpha_c = 0.950, \quad \alpha_t = 1.006,$$

$$|\alpha_d| = 1.039, \quad |\alpha_s| = 1.218, \quad |\alpha_b| = 0.790, \quad |\tilde{\alpha}_d| = 0.896, \quad |\tilde{\alpha}_s| = 0.822, \quad |\tilde{\alpha}_b| = 1.158, \tag{96}$$

we obtain the mixing angles and Dirac CP phase $\theta^q_{12} = 12.980°$, $\theta^q_{23} = 2.320°$, $\theta^q_{13} = 0.218°$, $\delta^q_{CP} = 64.216°$ compatible with the 3σ Global fit of CKMfitter [42] [see Eq. (69)]; the quark masses $m_d = 4.593$ MeV, $m_s = 103.819$ MeV, $m_b = 4.206$ GeV, $m_u = 2.164$ MeV, $m_c = 1.271$ GeV, and $m_t = 173.1$ GeV compatible with

the values in PDG [35] [see Eq. (70)]. Here, without loss of generality, the up-type quark masses m_u, m_c, and m_t are a one-to-one correspondence with α_u, α_c, and α_t, which have been taken real, and we have set $\arg(\alpha_b) = 0$.

The masses of the charged leptons m_e, m_μ, and m_τ are in a one-to-one correspondence with the real parameters α_e,
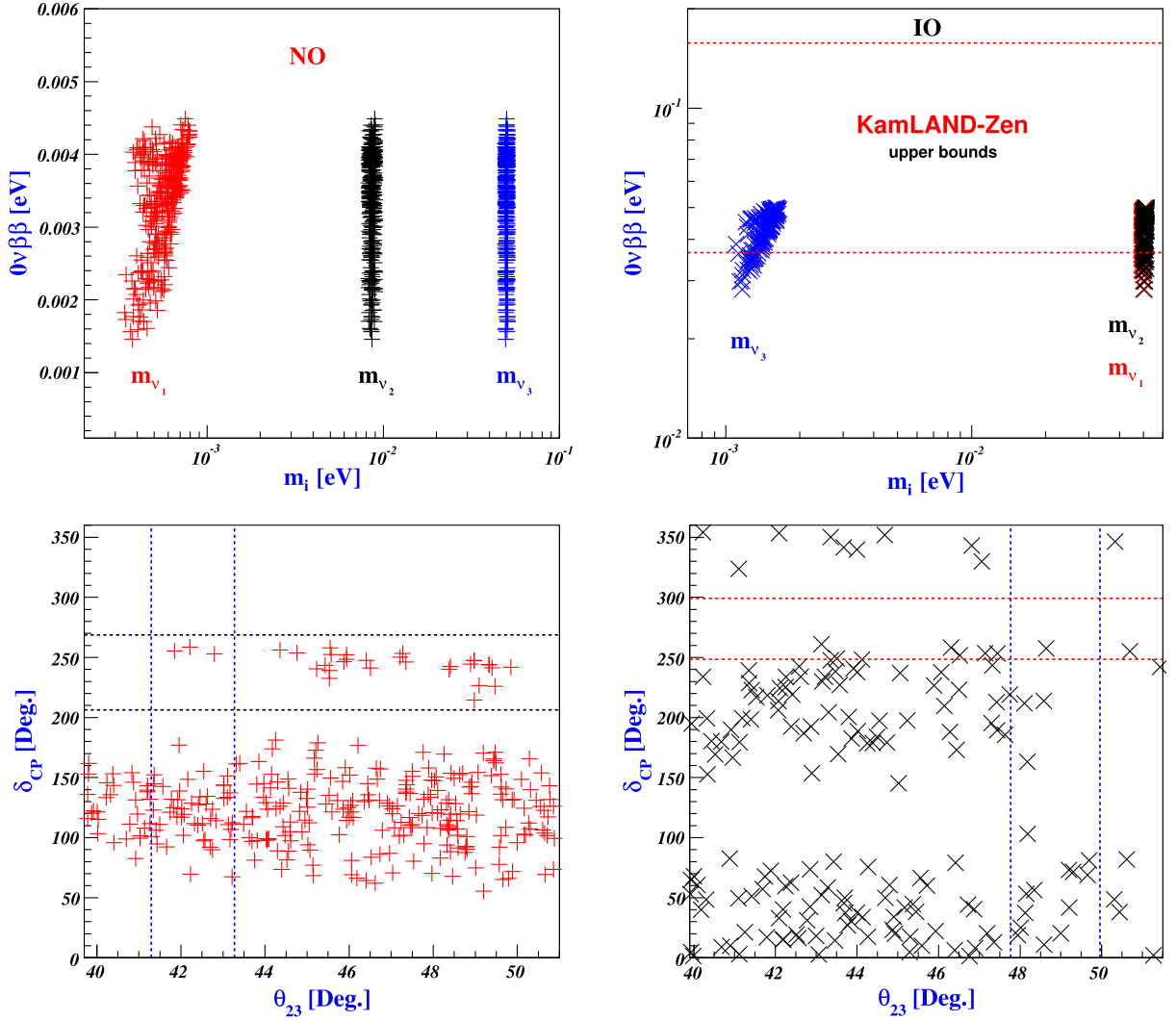
FIG. 4. Plots for $0\nu\beta\beta$-decay rate (upper panel) and leptonic Dirac CP phase δ_{CP} (lower panel) as a function of the neutrino masses m_{ν_i} and the atmospheric mixing angle θ_{23}, respectively, for NO (left) and IO (right). Vertical and horizontal dashed lines represent the 1σ bounds for θ_{23} and δ_{CP}, respectively, in Table III. Horizontal red lines indicate the upper bound of KamLAND-Zen result of Eq. (91) [65].

α_μ, and α_τ from Eq. (79). Using the numerical results of Eq. (95) from the quark sector, with the inputs

$$\alpha_e = 1.268 \quad \text{for } |f_e| = 20 \quad (\alpha_e = 0.757 \quad \text{for } |f_e| = 19),$$
$$\alpha_\mu = 0.900, \quad \alpha_\tau = 1.148, \tag{97}$$

we obtain the charged-lepton masses, which agree well with the empirical values of Eq. (80).

B. Neutrino

The seesaw mechanism in Eq. (87) operates at the $U(1)_X$ symmetry breakdown scale, while its implications are measured by experiments below the EW scale. Therefore, quantum corrections to neutrino masses and mixing angles can be crucial, especially for degenerate

neutrino masses [63]. However, based on our observation that the neutrino mass spectra exhibit hierarchy at the scale of $U(1)_X$ breakdown (as depicted in Fig. 4), we can safely assume that the renormalization group running effect on observables can be ignored.

Neutrino oscillation experiments currently aim to make precise measurements of the Dirac CP-violating phase δ_{CP} and atmospheric mixing angle θ_{23}. Using our model, we investigate which values of δ_{CP} and θ_{23} can predict the mass hierarchy of neutrinos (NO or IO) and identify observables that can be tested in current and next-generation experiments. To explore the parameter spaces, we scan the precision constraints $\{\theta_{13}, \theta_{23}, \theta_{12}, \Delta m^2_{\text{Sol}}, \Delta m^2_{\text{Atm}}\}$ at 3σ from Table III. Using the reference values from Eq. (95) in the quark and charged-lepton sectors, we determine the input parameter spaces of Eq. (93) for both NO and IO at the
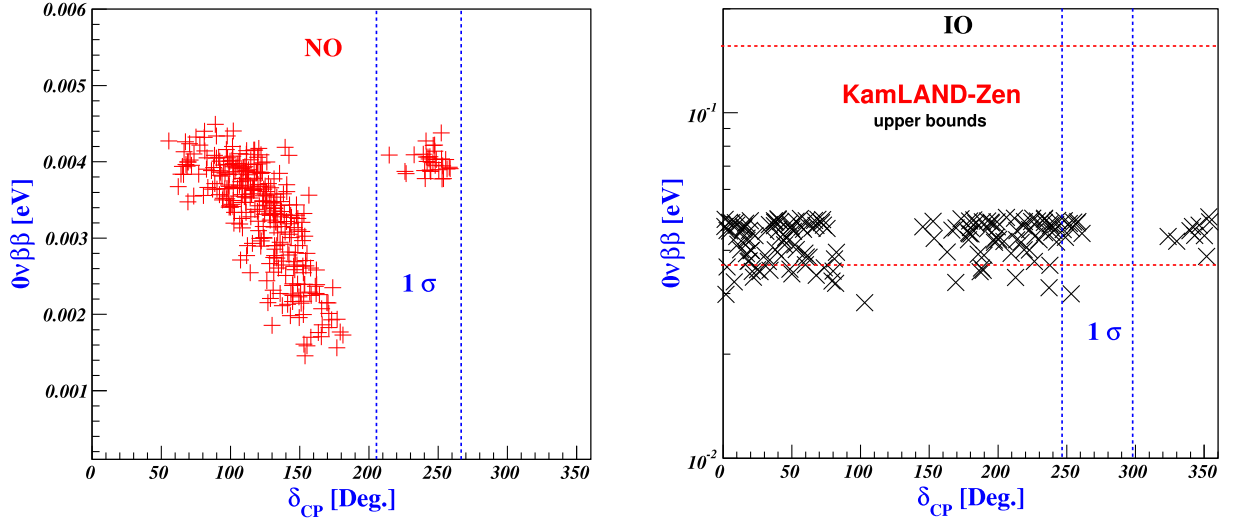
FIG. 5. Plots for $0\nu\beta\beta$-decay rate as a function of leptonic Dirac CP phase δ_{CP} for NO (left) and IO (right). Vertical dashed lines indicate the 1σ bound for δ_{CP} listed in Table III, while horizontal red lines represent the upper bound of KamLAND-Zen result of Eq. (91) [65] for the $0\nu\beta\beta$-decay rate.

$U(1)_X$-breaking scale, for example, taking $\langle\chi\rangle = 5 \times 10^{13}$ GeV (see Tables V, VI, and VII); for NO

$$\tilde{\beta}_2 = [0.48, 1.10], \qquad \tilde{\beta}_3 = [0.61, 1.18], \quad \arg(\tilde{\beta}_{2(3)}) = [0, 2\pi]$$
$$m_0\langle\chi\rangle/v_u^2 = [0.59, 1.84], \qquad \gamma = [0.37, 0.84], \qquad \gamma' = [0.37, 0.65]$$
$$\arg(\gamma) = [4.42, 5.55], \quad \arg(\gamma') = [1.30, 2.19], \tag{98}$$

where $\beta_1 = [0.97, 1.47]$, $\beta_2 = [0.61, 1.11]$, and $\beta_3 = [0.69, 1.15]$; and for IO

$$\tilde{\beta}_2 = [0.55, 0.87], \qquad \tilde{\beta}_3 = [0.56, 0.86], \quad \arg(\tilde{\beta}_{2(3)}) = [0, 2\pi]$$
$$m_0\langle\chi\rangle/v_u^2 = [0.81, 1.39], \qquad \gamma = [0.758, 1.154], \qquad \gamma' = [0.350, 0.618]$$
$$\arg(\gamma) = [2.92, 4.19], \quad \arg(\gamma') = [0.1, 1.29] \,\&\, [5.66, 6.26], \tag{99}$$

where $\beta_1 = [0.98, 1.29]$, $\beta_2 = [0.69, 0.95]$, and $\beta_3 = [0.68, 0.93]$. For these parameter regions, we investigate how the $0\nu\beta\beta$-decay rate and Dirac CP phase can be determined for the normal and inverted mass ordering. These predictions are represented by crosses and X marks for NO and IO, respectively, in Fig. 5. Referring to the two-dimensional allowed regions at 3σ presented in Ref. [61], we note that the most favored regions correspond to $\delta_{CP} \sim 250°$, whereas there are no favored regions with respect to θ_{23}. Ongoing experiments like DUNE [66], as well as proposed next-generation experiments such as Hyper-K [67], are poised to greatly reduce uncertainties in the values of θ_{23} and δ_{CP}, providing a rigorous test for our proposed model. Furthermore, ongoing and future experiments on $0\nu\beta\beta$ decay like NEXT [68], SNO+ [69], KamLAND-Zen [65], Theia [70], and SuperNEMO [71] may soon reach a sensitivity to exclude the inverted mass ordering of our model. In addition, the sum of the three neutrino masses, $\sum m_\nu = m_{\nu_1} + m_{\nu_2} + m_{\nu_3}$, can be

FIG. 6. Plot for $\sum m_\nu = m_{\nu_1} + m_{\nu_2} + m_{\nu_3}$ as a function of m_{lightest} for NO (red) and IO (black).

constrained by cosmological and astrophysical observations. The current upper bound on the sum of three neutrinos is given by $\sum m_\nu < 0.120$ eV at 95% C.L. for TT, TE, and EE + lowE + lensing + BAO [72]. The bound is obtained by assuming that neutrinos are stable on timescales of order the age of the Universe and gets weakened if neutrinos decay, so values of $\sum m_\nu$ as large as 0.9 eV are still by the data [73]. On the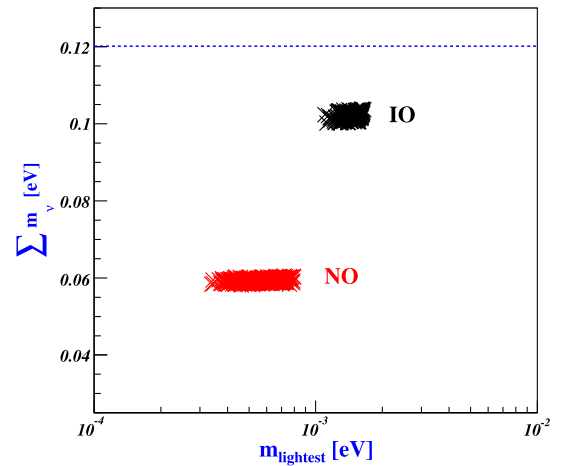 other hand, the sum of neutrino masses is predicted from the atmospheric and solar mass splittings when the lightest neutrino mass is fixed. Figure 6 represents the prediction of the sum of neutrino masses. From our numerical analysis carried out as described before, the lightest neutrino mass is constrained to be $0.0003397 \lesssim m_{\text{lightest}} = m_{\nu_1} \lesssim 0.0007945$ eV for the case of NO, which results in $0.0582 \lesssim \sum m_\nu \lesssim 0.0605$ eV. In contrast, for the case of IO, the sum of neutrino masses falls within the range of 0.1003 to 0.1038 eV. This range results from the constraint on the lightest neutrino mass, $0.001125 \lesssim m_{\text{lightest}} = m_{\nu_3} \lesssim 0.001647$ eV, which is obtained from our numerical analysis.

VI. CONCLUSION

We proposed a minimal extension of a modular-invariant model that incorporates sterile neutrinos and a QCD axion (as a strong candidate of dark matter) into the SM to account for the mass and mixing hierarchies of quarks and leptons, as well as the strong CP problem. Our model, based on the 4D effective action, features the $G_{\text{SM}} \times \Gamma_N \times U(1)_X$ symmetry. To ensure the reliability of our model, we have examined the modular forms of the superpotential, corrected by Kähler transformation, under the $G_{\text{SM}} \times \Gamma_N \times U(1)_X$ symmetry, while also considering the modular and $U(1)_X$ anomaly-free conditions. The model features a minimal set of fields that transform based on representations of $G_{\text{SM}} \times \Gamma_N \times U(1)_X$ and includes modular forms of level N. These modular forms act as Yukawa couplings and transform under the modular group Γ_N. Our numerical analysis guarantees that, in the supersymmetric limit, all Yukawa coefficients in the superpotential are complex numbers with a unit absolute value, implying a democratic distribution.

We demonstrated, as an explicit example, a level-3 modular form-induced superpotential by introducing minimal supermultiplets. The extension includes right-handed neutrinos (N^c) and SM gauge singlet scalar fields (χ and $\tilde{\chi}$) with zero modular weight and ($+$ and $-$) charge under $U(1)_X$. These scalar fields are crucial in generating the QCD axion, heavy neutrino mass, and fermion mass hierarchy. Modular invariance of both the superpotential and Kähler potential allows for Kähler transformation to correct modular form weight in the superpotential, enabling a τ-independent superpotential for the scalar potential. The sterile neutrinos are introduced to satisfy the $U(1)_X$-mixed gravitational anomaly-free condition, explain small active

neutrino masses via the seesaw mechanism, and provide a well-motivated PQ symmetry-breaking scale. As the fields $\chi(\tilde{\chi})$ have modular weights of 0, any additional correction terms arising from higher-weight modular forms are not permitted in the superpotentials. However, the combination $\chi\tilde{\chi}$ can trigger higher-order corrections that are permissible and do not modify the leading-order flavor structures. Taking into account both SUSY-breaking effects and supersymmetric next-leading-order Planck-suppressed terms, we have determined the low axion decay constant (or seesaw scale). This leads to an approximate range for the PQ scale $\langle \chi \rangle$ (equivalently, the seesaw scale) of 10^{13} to 10^{15} GeV for $m_{3/2}$ values between 1 and 10^6 TeV; see Tables V–VII. Interestingly enough, in our model, the PQ-breaking scale (or axion mass) is closely linked to the seesaw scale and the soft SUSY-breaking mass. Our model with E/N_C could be tested by ongoing experiments such as KLASH [33] and FLASH [34], see Figs. 1 and 2, by considering the scale of $U(1)_X$ breakdown.

We explored numerical values of physical parameters that satisfy the highly precise data on the mass of quarks and charged leptons, as well as the quark mixing angles, except for the quark Dirac CP phase. Our model predicts that the value of δ_{CP}^q falls within the range of 38° to 87°, which is consistent with experimental data. Notably, the effective Yukawa coefficients satisfying the experimental data fall well within the bound specified in Eq. (60), as shown in the top-left panel of Fig. 3. This suggests that our assumption, as stated in Eq. (2), that the Yukawa coefficients have a natural size of unity is plausible. Using precise neutrino oscillation data as constraints, we investigated how the $0\nu\beta\beta$-decay rate and Dirac CP phase could be determined for the normal and inverted mass ordering in the neutrino sector. Referring to the 3σ allowed regions in Ref. [61], we note that the most favored regions for our proposed model are $\delta_{CP} \sim 250°$, with no favored regions with respect to θ_{23}. Ongoing experiments, such as DUNE [66], and proposed next-generation experiments, such as Hyper-K [67], are expected to greatly reduce uncertainties in the values of θ_{23} and δ_{CP}, providing a rigorous test for our model. Additionally, ongoing and future experiments on $0\nu\beta\beta$ decay, such as NEXT [68], SNO+ [69], KamLAND-Zen [65], Theia [70], and SuperNEMO [71], may soon have the sensitivity to exclude the inverted mass ordering in our model.

APPENDIX A: THE GROUP A_4

The group A_4 is the symmetry group of the tetrahedron, isomorphic to the finite group of the even permutations of four objects. The group A_4 has two generators, denoted S and T, satisfying the relations $S^2 = T^3 = (ST)^3 = \mathbf{1}$. In the three-dimensional complex representation, S and T are given by

$$S = \frac{1}{3}\begin{pmatrix} -1 & 2 & 2 \\ 2 & -1 & 2 \\ 2 & 2 & -1 \end{pmatrix}, \qquad T = \begin{pmatrix} 1 & 0 & 0 \\ 0 & \omega & 0 \\ 0 & 0 & \omega^2 \end{pmatrix}, \quad (A1)$$

where $\omega = e^{i2\pi/3} = -1/2 + i\sqrt{3}/2$ is a complex cubic root of unity. A_4 has four irreducible representations: three singlets $\mathbf{1}, \mathbf{1}'$, and $\mathbf{1}''$ and one triplet $\mathbf{3}$. An A_4 singlet $\mathbf{a}$ is invariant under the action of S ($S\mathbf{a} = \mathbf{a}$), while the action of T produces $T\mathbf{a} = \mathbf{a}$ for $\mathbf{1}$, $T\mathbf{a} = \omega\mathbf{a}$ for $\mathbf{1}'$, and $T\mathbf{a} = \omega^2\mathbf{a}$ for $\mathbf{1}''$. Products of two A_4 representations decompose into irreducible representations according to the following

multiplication rules: $\mathbf{3} \otimes \mathbf{3} = \mathbf{3}_s \oplus \mathbf{3}_a \oplus \mathbf{1} \oplus \mathbf{1}' \oplus \mathbf{1}''$, $\mathbf{1}' \oplus \mathbf{1}' = \mathbf{1}''$, and $\mathbf{1}'' \oplus \mathbf{1}'' = \mathbf{1}'$. Explicitly, if (a_1, a_2, a_3) and (b_1, b_2, b_3) denote two A_4 triplets, then we have Eq. (30).

APPENDIX B: THE CKM MIXING MATRIX

The CKM mixing matrix is given in the Wolfenstein parametrization [39] by

$$V_{\text{CKM}} = \begin{pmatrix} 1 - \frac{1}{2}\lambda^2 & \lambda & A_d\lambda^3(\rho - i\eta) \\ -\lambda & 1 - \frac{1}{2}\lambda^2 & A_d\lambda^2 \\ A_d\lambda^3(1 - \rho - i\eta) & -A_d\lambda^2 & 1 \end{pmatrix}$$
$$+ \mathcal{O}(\lambda^4), \qquad (B1)$$

where $\lambda = 0.22500^{+0.00082}_{-0.00063}$, $A_d = 0.813^{+0.026}_{-0.018}$, $\bar{\rho} = \rho/(1 - \lambda^2/2) = 0.157^{+0.036}_{-0.018}$, and $\bar{\eta} = \eta/(1 - \lambda^2/2) = 0.347^{+0.030}_{-0.020}$ with 3σ errors [42].

TABLE V. The quark and lepton $U(1)_X$ quantum numbers that satisfy experimental results, including Eqs. (69), (70), and (74) and Table III as well as the $U(1)$-mixed gravitational anomaly-free condition for normal neutrino mass ordering. We present numerical results for QCD anomaly coefficient N_C, QCD axion decay constant F_a, QCD and QED anomaly ratio E/N_C, axion-electron coupling g_{ae} ($z = 0.47$), axion-photon coupling $g_{a\gamma\gamma}$ ($z = 0.47$), axion mass m_a, and branching ratio $\mathrm{Br}(K^+ \to \pi^+ + a) \equiv \mathrm{Br}(K\pi a)$.

$U(1)_X$	f_u	f_c	f_d	f_s	f_b	f_e	f_μ	f_τ	g_e	g_μ	g_τ	N_C	$\frac{F_a}{\text{GeV}}$	$\frac{E}{N_C}$	$\frac{g_{ae}}{10^{-17}}$	$\frac{\lvert g_{a\gamma\gamma}\rvert}{10^{-17}\,\text{GeV}^{-1}}$	$\frac{m_a}{10^{-7}\,\text{eV}}$	$\mathrm{Br}(K\pi a)$
	20	8	14	11	5	20	9	4	6	4	5							$4.2^{+1.9}_{-1.7} \times 10^{-15}$
I-a	$\mp$	$\pm$	$\pm$	$\mp$	$\pm$	$\pm$	$\mp$	$\pm$	$\pm$	$\mp$	$\mp$	± 4	5×10^{12}	$-\frac{5}{6}$	36.13	66.00	10.89	
I-b	$\mp$	$\pm$	$\pm$	$\mp$	$\pm$	$\pm$	$\mp$	$\mp$	$\pm$	$\pm$	$\mp$	± 4	5×10^{12}	$\frac{19}{6}$	36.13	26.94	10.89	
I-c	$\mp$	$\pm$	$\mp$	$\pm$	$\pm$	$\pm$	$\mp$	$\pm$	$\pm$	$\pm$	$\pm$	± 10	2×10^{12}	$\frac{1}{15}$	36.13	112.71	27.21	
I-d	$\mp$	$\pm$	$\mp$	$\pm$	$\pm$	$\pm$	$\pm$	$\mp$	$\pm$	$\pm$	$\mp$	± 10	2×10^{12}	$-\frac{29}{15}$	36.13	228.88	27.21	
I-e	$\mp$	$\pm$	$\mp$	$\pm$	$\pm$	$\pm$	$\pm$	$\pm$	$\pm$	$\mp$	$\mp$	± 10	2×10^{12}	$-\frac{53}{15}$	36.13	321.82	27.21	
	21	8	14	11	5	20	9	4	5	3	4							$4.2^{+1.9}_{-1.7} \times 10^{-15}$
II	$\mp$	$\pm$	$\pm$	$\mp$	$\mp$	$\pm$	$\pm$	$\pm$	$\pm$	$\pm$	$\pm$	± 15	1.3×10^{12}	-2	37.06	358.09	41.87	
	20	8	14	11	5	19	9	4	5	3	4							$1.7^{+0.8}_{-0.7} \times 10^{-16}$
III-a	$\mp$	$\pm$	$\pm$	$\mp$	$\pm$	$\pm$	$\mp$	$\mp$	$\pm$	$\mp$	$\pm$	± 4	2.5×10^{13}	$\frac{11}{3}$	6.87	7.71	2.18	
III-b	$\mp$	$\pm$	$\pm$	$\mp$	$\pm$	$\pm$	$\pm$	$\mp$	$\mp$	$\mp$	$\mp$	± 4	2.5×10^{13}	$-\frac{16}{3}$	6.87	34.11	2.18	
III-c	$\mp$	$\pm$	$\pm$	$\mp$	$\pm$	$\pm$	$\mp$	$\pm$	$\pm$	$\mp$	$\mp$	± 4	2.5×10^{13}	$-\frac{1}{3}$	6.87	10.88	2.18	
III-d	$\mp$	$\pm$	$\mp$	$\pm$	$\pm$	$\pm$	$\pm$	$\pm$	$\pm$	$\mp$	$\mp$	± 10	10^{13}	$-\frac{10}{3}$	6.87	62.04	5.44	
III-e	$\mp$	$\pm$	$\mp$	$\pm$	$\pm$	$\pm$	$\pm$	$\mp$	$\pm$	$\mp$	$\pm$	± 10	10^{13}	$-\frac{26}{15}$	6.87	43.45	5.44	
	20	8	14	11	5	20	9	4	4	2	3							$4.2^{+1.9}_{-1.7} \times 10^{-17}$
IV-a	$\mp$	$\pm$	$\pm$	$\mp$	$\pm$	$\pm$	$\mp$	$\pm$	$\mp$	$\mp$	$\pm$	± 4	5×10^{13}	$-\frac{5}{6}$	3.61	6.60	1.09	
IV-b	$\mp$	$\pm$	$\pm$	$\mp$	$\pm$	$\pm$	$\mp$	$\mp$	$\pm$	$\mp$	$\pm$	± 4	5×10^{13}	$\frac{19}{6}$	3.61	2.69	1.09	
IV-c	$\mp$	$\pm$	$\mp$	$\pm$	$\pm$	$\pm$	$\pm$	$\mp$	$\pm$	$\mp$	$\pm$	± 10	2×10^{13}	$-\frac{29}{15}$	3.61	22.89	2.72	
IV-d	$\mp$	$\pm$	$\mp$	$\pm$	$\pm$	$\pm$	$\pm$	$\mp$	$\mp$	$\mp$	$\pm$	± 10	2×10^{13}	$-\frac{53}{15}$	3.61	32.18	2.72	
IV-e	$\mp$	$\pm$	$\pm$	$\mp$	$\mp$	$\pm$	$\pm$	$\pm$	$\pm$	$\pm$	$\pm$	± 14	1.43×10^{13}	$-\frac{7}{3}$	3.61	35.30	3.81	

TABLE VI. The same as in Table V.

$U(1)_X$	f_u	f_c	f_d	f_s	f_b	f_e	f_μ	f_τ	g_e	g_μ	g_τ	N_C	$\frac{F_a}{\text{GeV}}$	$\frac{E}{N_C}$	$\frac{g_{ae}}{10^{-17}}$	$\frac{|g_{a\gamma\gamma}|}{10^{-17}\,\text{GeV}^{-1}}$	$\frac{m_a}{10^{-7}\,\text{eV}}$	$\text{Br}(K\pi a)$
	21	8	14	11	5	19	9	4	4	2	3							$4.2^{+1.9}_{-1.7}\times10^{-17}$
V-a	$\mp$	$\pm$	$\pm$	$\mp$	$\pm$	$\pm$	$\mp$	$\pm$	$\mp$	$\pm$	$\pm$	±5	4×10^{13}	$\frac{4}{15}$	3.43	5.05	1.36	
V-b	$\mp$	$\pm$	$\pm$	$\mp$	$\pm$	$\pm$	$\mp$	$\mp$	$\pm$	$\pm$	$\pm$	±5	4×10^{13}	$\frac{52}{15}$	3.43	4.24	1.36	
V-c	$\mp$	$\pm$	$\pm$	$\mp$	$\pm$	$\pm$	$\pm$	$\mp$	$\mp$	$\mp$	$\mp$	±5	4×10^{13}	$-\frac{56}{15}$	3.43	16.67	1.36	
V-d	$\mp$	$\pm$	$\mp$	$\pm$	$\pm$	$\pm$	$\pm$	$\pm$	$\mp$	$\pm$	$\pm$	±11	1.8×10^{13}	$-\frac{92}{33}$	3.43	30.64	2.99	
V-e	$\mp$	$\pm$	$\mp$	$\pm$	$\pm$	$\pm$	$\pm$	$\mp$	$\pm$	$\pm$	$\pm$	±11	1.8×10^{13}	$-\frac{4}{3}$	3.43	21.34	2.99	
	20	8	14	11	5	19	9	4	3	1	2							$1.7^{+0.8}_{-0.7}\times10^{-18}$
VI-a	$\mp$	$\pm$	$\pm$	$\mp$	$\pm$	$\pm$	$\mp$	$\pm$	$\mp$	$\mp$	$\pm$	±4	2.5×10^{14}	$-\frac{1}{3}$	0.69	1.09	0.22	
VI-b	$\mp$	$\pm$	$\pm$	$\mp$	$\pm$	$\pm$	$\mp$	$\mp$	$\pm$	$\pm$	$\pm$	±4	2.5×10^{14}	$\frac{11}{3}$	0.69	0.77	0.22	
VI-c	$\mp$	$\pm$	$\mp$	$\pm$	$\pm$	$\pm$	$\pm$	$\pm$	$\mp$	$\mp$	$\pm$	±10	10^{14}	$-\frac{10}{3}$	0.69	6.20	0.54	
VI-d	$\mp$	$\pm$	$\mp$	$\pm$	$\pm$	$\pm$	$\pm$	$\mp$	$\pm$	$\pm$	$\pm$	±10	10^{14}	$-\frac{26}{15}$	0.69	4.35	0.54	
	21	8	14	11	5	20	9	4	3	1	2							$1.7^{+0.8}_{-0.7}\times10^{-18}$
VII-a	$\mp$	$\pm$	$\pm$	$\mp$	$\pm$	$\pm$	$\mp$	$\pm$	$\mp$	$\pm$	$\pm$	±5	2×10^{14}	$-\frac{2}{15}$	0.72	1.24	0.27	
VII-b	$\mp$	$\pm$	$\mp$	$\pm$	$\pm$	$\pm$	$\pm$	$\pm$	$\pm$	$\mp$	$\mp$	±11	9×10^{13}	$-\frac{98}{33}$	0.72	6.36	0.60	
	21	8	14	11	5	19	9	4	2	0	1							$4.2^{+1.9}_{-1.7}\times10^{-19}$
VIII-a	$\mp$	$\pm$	$\pm$	$\mp$	$\pm$	$\pm$	$\mp$	$\pm$	$\pm$	0	$\mp$	±5	4×10^{14}	$\frac{4}{15}$	0.34	0.51	0.14	
VIII-b	$\mp$	$\pm$	$\mp$	$\pm$	$\pm$	$\pm$	$\pm$	$\pm$	$\pm$	0	$\mp$	±11	1.8×10^{14}	$-\frac{92}{33}$	0.34	3.06	0.30	
	20	8	14	11	5	20	9	4	2	0	1							$4.2^{+1.9}_{-1.7}\times10^{-19}$
IX-a	$\mp$	$\pm$	$\pm$	$\mp$	$\pm$	$\pm$	$\mp$	$\pm$	$\mp$	0	$\mp$	±4	5×10^{14}	$-\frac{5}{6}$	0.36	0.66	0.11	
IX-b	$\mp$	$\pm$	$\mp$	$\pm$	$\pm$	$\pm$	$\pm$	$\pm$	$\mp$	0	$\mp$	±10	2×10^{14}	$-\frac{53}{15}$	0.36	3.22	0.27	

TABLE VII. The same as in Table V, except for the inverted neutrino mass ordering.

$U(1)_X$	f_u	f_c	f_d	f_s	f_b	f_e	f_μ	f_τ	g_e	g_μ	g_τ	N_C	$\frac{F_a}{\text{GeV}}$	$\frac{E}{N_C}$	$\frac{g_{ae}}{10^{-17}}$	$\frac{|g_{a\gamma\gamma}|}{10^{-17}\,\text{GeV}^{-1}}$	$\frac{m_a}{10^{-7}\,\text{eV}}$	$\text{Br}(K\pi a)$
	19	8	14	11	5	20	9	4	2	3	3							$1.7^{+0.8}_{-0.7}\times10^{-16}$
I-a	$\mp$	$\pm$	$\pm$	$\mp$	$\pm$	$\pm$	$\mp$	$\mp$	$\pm$	$\substack{\mp\\\pm}$	$\substack{\pm\\\mp}$	±3	3.33×10^{13}	$\frac{10}{3}$	7.23	4.62	1.63	
I-b	$\mp$	$\pm$	$\mp$	$\pm$	$\pm$	$\pm$	$\pm$	$\mp$	$\pm$	$\substack{\mp\\\pm}$	$\substack{\pm\\\mp}$	±9	1.11×10^{13}	$-\frac{22}{9}$	7.23	46.54	4.90	
	20	8	14	11	5	19	9	4	2	3	3							$1.7^{+0.8}_{-0.7}\times10^{-16}$
II-a	$\mp$	$\pm$	$\pm$	$\mp$	$\pm$	$\pm$	$\mp$	$\pm$	$\mp$	$\substack{\mp\\\pm}$	$\substack{\pm\\\mp}$	±4	2.5×10^{13}	$-\frac{1}{3}$	6.87	10.88	2.18	
II-b	$\mp$	$\pm$	$\mp$	$\pm$	$\pm$	$\pm$	$\pm$	$\pm$	$\mp$	$\substack{\mp\\\pm}$	$\substack{\pm\\\mp}$	±10	10^{13}	$-\frac{10}{3}$	6.87	62.04	5.44	
	20	8	14	11	5	20	9	4	1	2	2							$4.2^{+1.9}_{-1.7}\times10^{-17}$
III-a	$\mp$	$\pm$	$\pm$	$\mp$	$\pm$	$\pm$	$\mp$	$\mp$	$\pm$	$\pm$	$\pm$	±4	5×10^{13}	$\frac{19}{6}$	3.61	6.60	1.09	
III-b	$\mp$	$\pm$	$\pm$	$\mp$	$\pm$	$\pm$	$\mp$	$\pm$	$\pm$	$\mp$	$\mp$	±4	5×10^{13}	$-\frac{5}{6}$	3.61	2.69	1.09	
III-c	$\mp$	$\pm$	$\mp$	$\pm$	$\pm$	$\pm$	$\mp$	$\pm$	$\pm$	$\pm$	$\pm$	±10	2×10^{13}	$-\frac{29}{15}$	3.61	22.89	2.72	
III-d	$\mp$	$\pm$	$\mp$	$\pm$	$\pm$	$\pm$	$\pm$	$\pm$	$\pm$	$\mp$	$\mp$	±10	2×10^{13}	$-\frac{53}{15}$	3.61	32.18	2.72	
	19	8	14	11	5	19	9	4	1	2	2							$4.2^{+1.9}_{-1.7}\times10^{-17}$
IV-a	$\mp$	$\pm$	$\pm$	$\mp$	$\pm$	$\pm$	$\mp$	$\mp$	$\mp$	$\pm$	$\pm$	±3	6.67×10^{13}	4	3.43	3.47	8.16	
IV-b	$\mp$	$\pm$	$\pm$	$\mp$	$\pm$	$\pm$	$\mp$	$\pm$	$\mp$	$\mp$	$\mp$	±3	6.67×10^{13}	$-\frac{4}{3}$	3.43	5.82	8.16	
IV-c	$\mp$	$\pm$	$\mp$	$\pm$	$\pm$	$\pm$	$\pm$	$\mp$	$\mp$	$\pm$	$\pm$	±9	2.22×10^{13}	$-\frac{20}{9}$	3.43	22.11	2.45	
IV-d	$\mp$	$\pm$	$\mp$	$\pm$	$\pm$	$\pm$	$\pm$	$\pm$	$\mp$	$\mp$	$\mp$	±9	2.22×10^{13}	-4	3.43	31.40	2.45	
	19	8	14	11	5	20	9	4	0	1	1							$1.7^{+0.8}_{-0.7}\times10^{-18}$
V-a	$\mp$	$\pm$	$\pm$	$\mp$	$\pm$	$\pm$	$\mp$	$\mp$	0	$\pm$	$\pm$	±3	3.33×10^{14}	$\frac{10}{3}$	0.72	0.46	0.16	
V-b	$\mp$	$\pm$	$\mp$	$\pm$	$\pm$	$\pm$	$\pm$	$\mp$	0	$\pm$	$\pm$	±9	1.11×10^{14}	$-\frac{22}{9}$	0.72	4.65	0.49	

[1] P. Minkowski, Phys. Lett. **67B**, 421 (1977); T. Yanagida, in *Proceedings of the Workshop on Unified Theories and Baryon Number in the Universe*, edited by O. Sawada and A. Sugamoto (KEK, Japan, 1979), Vol. 95; M. Gell-Mann, P. Ramond, and R. Slansky, in *Supergravity*, edited by P. Nieuwenhuizen and D. Freeman (North Holland, Amsterdam, 1979); R. N. Mohapatra and G. Senjanovic, Phys. Rev. Lett. **44**, 912 (1980).

[2] R. D. Peccei and H. R. Quinn, Phys. Rev. Lett. **38**, 1440 (1977); Phys. Rev. D **16**, 1791 (1977).

[3] F. Feruglio, arXiv:1706.08749.

[4] S. Ferrara, D. Lust, A. D. Shapere, and S. Theisen, Phys. Lett. B **225**, 363 (1989); S. Ferrara, D. Lust, and S. Theisen, Phys. Lett. B **233**, 147 (1989).

[5] T. Kobayashi, N. Omoto, Y. Shimizu, K. Takagi, M. Tanimoto, and T. H. Tatsuishi, J. High Energy Phys. 11 (2018) 196; S. J. D. King and S. F. King, J. High Energy Phys. 09 (2020) 043; F. J. de Anda, S. F. King, and E. Perdomo, Phys. Rev. D **101**, 015028 (2020); C. Y. Yao, J. N. Lu, and G. J. Ding, J. High Energy Phys. 05 (2021) 102; H. Okada and M. Tanimoto, Eur. Phys. J. C **81**, 52 (2021); C. Y. Yao, J. N. Lu, and G. J. Ding, J. High Energy Phys. 05 (2021) 102; S. Kikuchi, T. Kobayashi, H. Otsuka, M. Tanimoto, H. Uchida, and K. Yamamoto, Phys. Rev. D **106**, 035001 (2022); K. Hoshiya, S. Kikuchi, T. Kobayashi, and H. Uchida, Phys. Rev. D **106**, 115003 (2022); A. Baur, H. P. Nilles, S. Ramos-Sanchez, A. Trautner, and P. K. S. Vaudrevange, J. High Energy Phys. 09 (2022) 224; X. K. Du and F. Wang, J. High Energy Phys. 01 (2023) 036; Y. Abe, T. Higaki, J. Kawamura, and T. Kobayashi, arXiv:2302.11183; H. Okada and M. Tanimoto, Phys. Dark Universe **40**, 101204 (2023); S. T. Petcov and M. Tanimoto, arXiv:2306.05730; S. T. Petcov and M. Tanimoto, arXiv:2212.13336.

[6] G. J. Ding, S. F. King, and X. G. Liu, J. High Energy Phys. 09 (2019) 074; Y. H. Ahn, S. K. Kang, R. Ramos, and M. Tanimoto, Phys. Rev. D **106**, 095002 (2022).

[7] F. Feruglio, A. Strumia, and A. Titov, J. High Energy Phys. 07 (2023) 027.

[8] T. Kobayashi and H. Otsuka, Phys. Lett. B **807**, 135554 (2020).

[9] R. de Adelhart Toorop, F. Feruglio, and C. Hagedorn, Nucl. Phys. **B858**, 437 (2012).

[10] L. E. Ibanez and A. M. Uranga, *String Theory and Particle Physics: An Introduction to String Phenomenology* (Cambridge University Press, Cambridge, England, 2012).

[11] J. P. Derendinger, S. Ferrara, C. Kounnas, and F. Zwirner, Nucl. Phys. **B372**, 145 (1992).

[12] M. Dine, N. Seiberg, and E. Witten, Nucl. Phys. **B289**, 589 (1987); P. Svrcek and E. Witten, J. High Energy Phys. 06 (2006) 051.

[13] M. B. Green and J. H. Schwarz, Phys. Lett. **149B**, 117 (1984); Nucl. Phys. **B255**, 93 (1985); M. B. Green, J. H. Schwarz, and P. C. West, Nucl. Phys. **B254**, 327 (1985).

[14] C. P. Burgess, R. Kalosh, and F. Quevedo, J. High Energy Phys. 10 (2003) 056.

[15] D. V. Nanopoulos, K. A. Olive, M. Srednicki, and K. Tamvakis, Phys. Lett. **124B**, 171 (1983); H. Murayama, H. Suzuki, and T. Yanagida, Phys. Lett. B **291**, 418 (1992);

K. Choi, E. J. Chun, and J. E. Kim, Phys. Lett. B **403**, 209 (1997).

[16] Y. H. Ahn, Phys. Rev. D **100**, 015002 (2019).

[17] Y. H. Ahn, Phys. Rev. D **96**, 015022 (2017).

[18] Y. H. Ahn, Phys. Rev. D **91**, 056005 (2015).

[19] M. Kamionkowski and J. March-Russell, Phys. Lett. B **282**, 137 (1992); R. Kalosh, A. D. Linde, D. A. Linde, and L. Susskind, Phys. Rev. D **52**, 912 (1995); G. Dvali, arXiv:hep-th/0507215.

[20] Y. H. Ahn, Phys. Rev. D **98**, 035047 (2018); Y. H. Ahn, Nucl. Phys. **B939**, 534 (2019); Y. H. Ahn and X. Bi, Nucl. Phys. **B960**, 115210 (2020).

[21] Y. H. Ahn, S. K. Kang, and H. M. Lee, Phys. Rev. D **106**, 075029 (2022).

[22] S. Gukov, C. Vafa, and E. Witten, Nucl. Phys. **B584**, 69 (2000); **B608**, 477(E) (2001).

[23] S. B. Giddings, S. Kachru, and J. Polchinski, Phys. Rev. D **66**, 106006 (2002).

[24] K. Dasgupta, G. Rajesh, and S. Sethi, J. High Energy Phys. 08 (1999) 023.

[25] D. Cremades, L. E. Ibanez, and F. Marchesano, J. High Energy Phys. 07 (2003) 038; R. Blumenhagen, M. Cvetic, P. Langacker, and G. Shiu, Annu. Rev. Nucl. Part. Sci. **55**, 71 (2005); S. A. Abel and M. D. Goodsell, J. High Energy Phys. 10 (2007) 034; R. Blumenhagen, B. Kors, D. Lust, and S. Stieberger, Phys. Rep. **445**, 1 (2007); F. Marchesano, Fortschr. Phys. **55**, 491 (2007); I. Antoniadis, A. Kumar, and B. Panda, Nucl. Phys. **B823**, 116 (2009); T. Kobayashi, S. Nagamoto, and S. Uemura, Prog. Theor. Exp. Phys. **2017**, 023B02 (2017).

[26] D. Cremades, L. E. Ibanez, and F. Marchesano, J. High Energy Phys. 05 (2004) 079.

[27] A. Sagnotti, Phys. Lett. B **294**, 196 (1992).

[28] L. E. Ibanez, R. Rabadan, and A. M. Uranga, Nucl. Phys. **B542**, 112 (1999).

[29] E. Poppitz, Nucl. Phys. **B542**, 31 (1999).

[30] Z. Lalak, S. Lavignac, and H. P. Nilles, Nucl. Phys. **B559**, 48 (1999).

[31] Y. H. Ahn, Phys. Rev. D **93**, 085026 (2016).

[32] A. Achucarro, B. de Carlos, J. A. Casas, and L. Doplicher, J. High Energy Phys. 06 (2006) 014; E. Dudas and Y. Mambrini, J. High Energy Phys. 10 (2006) 044.

[33] D. Alesini, D. Babusci, P. Beltrame S. J., F. Björkeroth, F. Bossi, P. Ciambrone, G. Delle Monache, D. Di Gioacchino, P. Falferi, A. Gallo *et al.*, arXiv:1911.02427.

[34] C. Gatti, P. Gianotti, C. Ligi, M. Raggi, and P. Valente, Universe **7**, 236 (2021).

[35] R. L. Workman *et al.* (Particle Data Group), Prog. Theor. Exp. Phys. **2022**, 083C01 (2022).

[36] E. Ma and G. Rajasekaran, Phys. Rev. D **64**, 113012 (2001); G. Altarelli and F. Feruglio, Nucl. Phys. **B720**, 64 (2005); P. F. Harrison and W. G. Scott, Phys. Lett. B **557**, 76 (2003); X. G. He, Y. Y. Keum, and R. R. Volkas, J. High Energy Phys. 04 (2006) 039.

[37] Y. H. Ahn, S. Baek, and P. Gondolo, Phys. Rev. D **86**, 053004 (2012); Y. H. Ahn, S. K. Kang, and C. S. Kim, Phys. Rev. D **87**, 113012 (2013); Z. z. Xing, Phys. Lett. B **533**, 85 (2002); S. K. Kang, Z. z. Xing, and S. Zhou, Phys. Rev. D **73**, 013001 (2006); S. Chang, S. K. Kang, and K. Siyeon, Phys. Lett. B **597**, 78 (2004).

[38] Y. H. Ahn, H. Y. Cheng, and S. Oh, Phys. Rev. D **83**, 076012 (2011).

[39] L. Wolfenstein, Phys. Rev. Lett. **51**, 1945 (1983).

[40] Y. H. Ahn, H. Y. Cheng, and S. Oh, Phys. Lett. B **703**, 571 (2011).

[41] L. L. Chau and W. Y. Keung, Phys. Rev. Lett. **53**, 1802 (1984).

[42] http://ckmfitter.in2p3.fr.

[43] R. D. Bolton *et al.*, Phys. Rev. D **38**, 2077 (1988).

[44] A. V. Artamonov *et al.* (E949 Collaboration), Phys. Rev. Lett. **101**, 191802 (2008).

[45] A. Davidson and K. C. Wali, Phys. Rev. Lett. **48**, 11 (1982); F. Wilczek, Phys. Rev. Lett. **49**, 1549 (1982).

[46] J. L. Feng, T. Moroi, H. Murayama, and E. Schnapka, Phys. Rev. D **57**, 5875 (1998).

[47] Z. G. Berezhiani and M. Y. Khlopov, Sov. J. Nucl. Phys. **51**, 739 (1990); Z. Phys. C **49**, 73 (1991); A. S. Sakharov and M. Y. Khlopov, Phys. At. Nucl. **57**, 651 (1994).

[48] E. Cortina Gil *et al.* (NA62 Collaboration), J. High Energy Phys. 06 (2021) 093.

[49] A. Ayala, I. DomÃnguez, M. Giannotti, A. Mirizzi, and O. Straniero, Phys. Rev. Lett. **113**, 191302 (2014).

[50] J. Redondo, J. Cosmol. Astropart. Phys. 12 (2013) 008.

[51] N. Viaux, M. Catelan, P. B. Stetson, G. Raffelt, J. Redondo, A. A. R. Valcarce, and A. Weiss, Astron. Astrophys. **558**, A12 (2013); N. Viaux, M. Catelan, P. B. Stetson, G. Raffelt, J. Redondo, A. A. R. Valcarce, and A. Weiss, Phys. Rev. Lett. **111**, 231301 (2013).

[52] M. M. Miller Bertolami, B. E. Melendez, L. G. Althaus, and J. Isern, J. Cosmol. Astropart. Phys. 10 (2014) 069.

[53] J. Isern, E. Garcia-Berro, S. Torres, and S. Catalan, Astrophys. J. **682**, L109 (2008); J. Isern, S. Catalan, E. Garcia-Berro, and S. Torres, J. Phys. Conf. Ser. **172**, 012005 (2009); J. Isern, M. Hernanz, and E. Garcia-Berro, Astrophys. J. **392**, L23 (1992).

[54] S. DeGennaro, T. von Hippel, D. E. Winget, S. O. Kepler, A. Nitta, D. Koester, and L. Althaus, Astron. J. **135**, 1 (2008).

[55] N. Rowell and N. Hambly, arXiv:1102.3193.

[56] G. G. Raffelt, Phys. Lett. B **166**, 402 (1986); S. I. Blinnikov and N. V. Dunina-Barkovskaya, Mon. Not. R. Astron. Soc. **266**, 289 (1994).

[57] L. Wolfenstein, Phys. Rev. D **17**, 2369 (1978); S. P. Mikheyev and A. Y. Smirnov, Yad. Fiz. **42**, 1441 (1985) [Sov. J. Nucl. Phys. **42**, 913 (1985)].

[58] I. Esteban, M. C. Gonzalez-Garcia, A. Hernandez-Cabezudo, M. Maltoni, and T. Schwetz, J. High Energy Phys. 01 (2019) 106.

[59] P. F. de Salas, D. V. Forero, C. A. Ternes, M. Tortola, and J. W. F. Valle, Phys. Lett. B **782**, 633 (2018).

[60] F. Capozzi, E. Lisi, A. Marrone, and A. Palazzo, Prog. Part. Nucl. Phys. **102**, 48 (2018).

[61] I. Esteban, M. C. Gonzalez-Garcia, M. Maltoni, T. Schwetz, and A. Zhou, J. High Energy Phys. 09 (2020) 178; NuFIT 5.2 (2022), www.nu-fit.org.

[62] S. A. Kharusi, G. Anton, I. Badhrees, P. S. Barbeau, D. Beck, V. Belov, T. Bhatta, M. Breidenbach, T. Brunner, G. F. Cao *et al.*, Phys. Rev. D **104**, 112002 (2021).

[63] S. Antusch, J. Kersten, M. Lindner, M. Ratz, and M. A. Schmidt, J. High Energy Phys. 03 (2005) 024.

[64] S. J. Asztalos *et al.* (ADMX Collaboration), Phys. Rev. Lett. **104**, 041301 (2010).

[65] S. Abe *et al.* (KamLAND-Zen Collaboration), Phys. Rev. Lett. **130**, 051801 (2023).

[66] B. Abi *et al.* (DUNE Collaboration), arXiv:1807.10334.

[67] K. Abe *et al.* (Hyper-Kamiokande Collaboration), arXiv:1805.04163.

[68] C. Adams *et al.* (NEXT Collaboration), J. High Energy Phys. 08 (2021) 164.

[69] A. Allega *et al.* (SNO+ Collaboration), Phys. Rev. D **105**, 112012 (2022).

[70] M. Askins *et al.* (Theia Collaboration), Eur. Phys. J. C **80**, 416 (2020).

[71] R. Arnold, C. Augier, A. M. Bakalyarov, J. Baker, A. Barabash, P. Bernaudin, M. Bouchel, V. Brudanin, A. J. Caffrey, J. Cailleret *et al.*, Nucl. Instrum. Methods Phys. Res., Sect. A **536**, 79 (2005).

[72] N. Aghanim *et al.* (Planck Collaboration), Astron. Astrophys. **641**, A6 (2020); **652**, C4(E) (2021).

[73] Z. Chacko, A. Dev, P. Du, V. Poulin, and Y. Tsai, J. High Energy Phys. 04 (2020) 020.